



---

# Sediment transport and accumulation in Western Port

Report on Phase I of a study determining the sources  
of sediment to Western Port

Gary J. Hancock, Jon M. Olley and Peter J. Wallbrink

---

CSIRO Land and Water, Environmental Hydrology, Canberra  
Technical Report 47/01, November 2001

---



---

# Sediment transport and accumulation in Western Port

Report on Phase I of a study determining the sources  
of sediment to Western Port

Gary J. Hancock, Jon M. Olley and Peter J. Wallbrink

---

CSIRO Land and Water, Environmental Hydrology, Canberra  
Technical Report 47/01, November 2001

---

**Copyright**

© 2001 CSIRO Land and Water.

To the extent permitted by law, all rights are reserved and no part of this publication covered by copyright may be reproduced or copied in any form or by any means except with the written permission of CSIRO Land and Water.

**Important Disclaimer**

To the extent permitted by law, CSIRO Land and Water (including its employees and consultants) excludes all liability to any person for any consequences, including but not limited to all losses, damages, costs, expenses and any other compensation, arising directly or indirectly from using this publication (in part or in whole) and any information or material contained in it.

This report should be referenced as:

Hancock, G.J., Olley, J.M. and Wallbrink, P.J. (2001). Sediment transport and accumulation in Westernport. CSIRO Land and Water technical report 47/01.

## Executive Summary

Sediment accumulation and transport has been assessed in the north, east and southern regions of Western Port by examining the dynamics of sediment transport in the bay, and estimating the rate of sediment accumulation. Sediment transport was studied by determining the bay-wide spatial distribution of various particle size fractions, and estimating suspended particle residence times by measurements of  $^{234}\text{Th}$  uptake. Sediment accumulation was studied by determining sediment chronologies using fallout radionuclides ( $^{210}\text{Pb}$ ,  $^{137}\text{Cs}$ ), Pinus pollen and optically stimulated luminescence (OSL) dating. Measurements of major and trace elements were also made in an attempt to establish proxy age horizons distinguished by changes to sediment characteristics resulting from recent human activities.

Suspended particle residence times are short, and generally less than 1 day. This information indicates a dynamic system of sediment resuspension and redeposition of fine-grained sediment induced by tidal action. The pattern of fine-grained ( $<63\ \mu\text{m}$ ) sediment distribution in the bay, together with sediment core inventories of excess  $^{210}\text{Pb}$  and  $^{137}\text{Cs}$  activities indicate that net transport of fine-grained sediment is in a general southwards direction clock-wise around the bay, such that fine-grained sediment is being mobilised in the Upper North Arm, and focussed in the Rhyll (East Basin) and Corinella segments of the East Arm. Comparison of the distribution of fine-grained sediment determined by this study with that determined in the mid 1970's (Marsden and Mallet, 1975; Marsden et al., 1979) indicates a reduction in areal concentration of fine-grained sediment in the upper north arm over the last 25 year. The loss of fine is consistent with the observed particle size-distribution of the upper layers of sediment cores, which show highest sand content in Upper North Arm sites and highest silt/clay content in East Arm sites.

Profiles of  $^{210}\text{Pb}$  indicate that fine-grained sediment in the East Arm is mixed to a depth of at least 18 cm. A simple 2-layer mixing model was applied to the  $^{210}\text{Pb}$  profiles, where mixing below the upper mixed layer is assumed negligible. The model yielded an apparent mean accumulation rate of  $0.48\ \text{cm yr}^{-1}$  (equivalent to  $2.5\ \text{kg m}^{-2}\ \text{yr}^{-1}$  of dry sediment) for the southern-most site of the bay (East Basin). The apparent accumulation rate at the southern-most site in the Corinella segment is  $0.21\ \text{cm yr}^{-1}$ . Cs-137 profiles are consistent with these rates. These accumulation rates represent an average of the last 60 years, and are considered upper limits due to the possibility of slow vertical mixing of sediment below 20 cm depth. Approximate depositional loads of fine-grained sediment in the East Arm are estimated by extrapolating the  $^{210}\text{Pb}$  accumulation rates to the areas of clay-dominated sediment of the East Basin and Corinella segment. The calculated load lies between  $70$  and  $100\ \text{kt yr}^{-1}$  of dry sediment.

In the Upper North Arm sediment deposition over the last 40-60 years is confined to a sediment layer 12 to 24 cm thick. Due to the possibility of post-depositional mixing, the sediment deposition rate determined from this chronology ( $0.3$ - $0.4\ \text{cm yr}^{-1}$ ) is an upper limit. Despite the fact that recent sediment accumulation rates at most sites in the bay are less than  $0.5\ \text{cm yr}^{-1}$ , there are areas where sediment accumulation rates have been much higher. At one site in the Corinella segment more than 60 cm has been deposited over the last 40 years, equivalent to an accumulation rate of  $1.6\ \text{cm yr}^{-1}$ . This site illustrates the dynamic nature of sediment movement in some areas of the bay.

In the northern and eastern areas of the bay the particle size distribution of sediment is highly variable both laterally and vertically. In the northern sites cores show a general trend of increasing sand content over a period of time extending beyond the last 40 years. This trend could be due to an increasing rate of sand delivery to the bay, an increasing rate of fine sediment removal (resuspension) from Upper North Arm sediments, or a combination of both processes.

All cores show evidence for higher concentrations of P (50-100%) in the upper layer of sediment, corresponding to sediment delivered during the last 40 years. This may be due to an increase in the P load delivered to the bay, or the presence of higher levels of organic matter in the upper sediments (this is being investigated further). Trace element profiles do not show elevated levels of any metal in the upper layer. However, elevated levels of Cu and Mo are seen in sediment older than 40 years. It is likely that these concentration changes are a result of diagenesis (formation of sulphide minerals) rather than anthropogenic input.

## **Acknowledgements**

This study is jointly funded by Melbourne Water, CSIRO Land and Water and the Environmental Protection Agency (EPA) of Victoria.

We thank the following for their help with sample collection and for providing helpful information and discussions on Western Port; Neil Biggins, Andy Steven, Andy Stephens, Doug Newton (EPA), Rhys Coleman and Graham Rooney (Melbourne Water).

Danny Hunt, Haralds Alksnis and Carol Kelly (CSIRO) helped with sample collection, preparation and radionuclide analysis. Ralph Ogden (CSIRO) provided advice on pollen analysis. Heinz Buettikofer and Andrew Hughes (CSIRO) assisted with the preparation of some of the figures in this report.

## **Table of Contents**

<b>1. Introduction</b>	1
<b>2. Methods</b>	2
2.1 Sample collection	2
2.2 Analytical procedures	5
2.3 Tracers and chronometers	9
<b>3. Sediment transport and Distribution</b>	12
3.1 Suspended particle residence time	12
3.2 Sediment distribution	14
3.3 Excess <sup>210</sup> Pb and <sup>137</sup> Cs inventories	17
3.4 Discussion and summary of sediment transport and distribution	18
<b>4. Sediment Accumulation</b>	19
4.1 Application of chronological methods	19
4.2 Core chronologies	29
4.3 Trace elements	33
<b>5. Discussion</b>	35
5.1 East Arm sites	35
5.2 Upper North Arm sites	37
<b>6. Summary and Conclusions</b>	38
<b>References</b>	39
<b>Appendix</b>	42

## 1. Introduction

This report presents the findings of Phase 1 of a three year study to determine the primary sources of sediment to Western Port. The study was initiated by Melbourne Water to enable more effective setting of priorities for catchment rehabilitation. At the time of the study links have been proposed between sediment delivery to the bay and loss of a significant area of seagrass since the early 1970's. Although not the focus of the study, it is anticipated that a reduced sediment load is likely to benefit seagrass communities, and an increased understanding of sediment dynamics within the bay is likely to benefit seagrass restoration efforts.

The study is divided into three Phases. The main aim of Phase 1 is to determine the accumulation rate of sediment in Western Port over the last 100 years, particularly in areas most affected by seagrass loss. By doing this, the study aims to establish a history of sediment delivery to the bay, and determine whether sediment sources have changed significantly since European settlement. The sediment accumulation and sediment geochemistry data presented in this report will also be used in Phase 3 of the study, aimed at determining catchment sources.

The Westernport catchment has undergone significant change since European settlement due to land clearing and drainage of the Koo-wee-rup swamp. Soil and river bank erosion caused by these changes is believed to have significantly increased sediment loads into the Western Port marine environment (Sargeant, 1977). Wilk et al. (1979) examined the stratigraphy of a series of sediment cores collected in the late 1970's from the Upper North Arm of the bay. In areas denuded of seagrass the cores showed evidence of 3-5 cm of catchment-derived sediment overlying prior seagrass beds. Wilk et al. concluded that sufficient soil had been removed from the catchment since the swamp had been drained to more than cover the denuded area.

Current estimates of the sediment load delivered to Westernport are mainly based on limited periods of monitoring of suspended sediment and flow of rivers and streams entering the bay. Monitoring is typically limited to monthly measurements, and spans no more than 20 years. Sargeant (1977) estimated a total sediment load of  $99,000 \text{ m}^3 \text{ yr}^{-1}$  (equivalent to about  $60 \text{ kt yr}^{-1}$  dry weight) based on monitoring from 1973-1976. May and Stephens (1996) summarised data collected between 1973 and 1985 (from CEE, 1986). By summing the data a mean load of about  $40 \text{ kt yr}^{-1}$  is determined. Using a longer time series Lowe (1999) provided annual estimates of load for streams entering the northern area of the bay, ranging from  $24\text{-}37 \text{ kt yr}^{-1}$ .

However, it is well known that monitoring over limited periods of time does not necessarily yield accurate long-term sediment load estimates, particularly in Australian catchments where sporadic periods of high river flow deliver disproportionately high sediment loads (Olive et al., 1995). The use of catchment yields to estimate sediment accumulation in the bay is also affected by uncertainties in the efficiency of sediment delivery to the bay, sediment movement within the bay, and export of sediment to the sea. The significance of each of these factors on the sediment budget of the bay is largely unknown. In shallow coastal waters dominated by tidal currents significant relocation and focussing of sediment deposits is likely.

This report assesses the extent of sediment transport and accumulation in the north, east and south-east regions of the bay. This is done by

- i) examining the particle size distribution of sediment in the bay
- ii) assessing the dynamics of suspended particle resuspension using  $^{234}\text{Th}$  uptake, and relating it to the particle size distribution
- iii) establishing chronologies for sediment profiles from key areas of the bay using fallout radionuclides, OSL dating, *pinus* pollen measurements,

i) and ii) can allow an assessment of the transport pathways of fine-grained sediment in the bay, information which may have implications for the source of turbidity in the Bay. Sediment core chronologies can allow estimates of sediment accumulation and an assessment of the changing nature of bed stratum over recent decades.

## 2. Methods

### 2.1 Sample collection

Sediment core and water samples were collected from 8 sites during May 2 to May 4, 2000. Sample site locations are shown in Fig. 1, and sample collection details are given in Table 1. Sediment cores were collected by divers from 7 of the sites, mainly along the northern and eastern sides of the bay. Four sites lie within the North Arm of the bay incorporating the embayment head of Western Port. This segment is described as the Upper North Arm (Fig. 1). Three sites lie in the East Arm of the bay, including the Corinella segment (2) and the East Basin (1). Sites were selected adjacent to river and stream inputs, within areas of seagrass loss, and within zones of fine-grained sediment deposition.

Sediment cores were collected in two types of core tubes; 'short' polycarbonate tubes 100 mm in diameter, and 'long' PVC tubes 50 mm in diameter. The wider polycarbonate tubes were pushed into the sediment by the divers, and the PVC tubes were driven in using a drop-hammer device. The polycarbonate tubes yielded cores up to 60 cm long, and the drop-hammer device recovered cores up to 160 cm long. Cores were retrieved in an upright position, and placed upright in dry ice until frozen. The cores remained frozen until required for analysis.

Filtered water and suspended particulates  $>0.5 \mu\text{m}$  were collected at 7 of the sites. Between 450 and 700 L of water was pumped through a  $0.5 \mu\text{m}$  (nominal) polypropylene (PP) 25 cm cartridge filter (CUNO) at a flow rate of about 12 L/min. The cartridges and particles retained therein were kept for analysis. Filtered and unfiltered water (2 L) was also retained for suspended sediment analysis and radionuclide analysis.

Dissolved ( $<0.5 \mu\text{m}$ )  $^{234}\text{Th}$  was collected using a 25 cm cellulose melamine cartridge (CUNO Microkleen,  $5 \mu\text{m}$  nominal pore size) impregnated with  $\text{MnO}_2$ . This cartridge was placed in line with the PP filter cartridge so dissolved radionuclides passing through the PP cartridge filter were scavenged by the  $\text{MnO}_2$ . All cartridges were placed into clean plastic bags and returned to the laboratory for analysis.

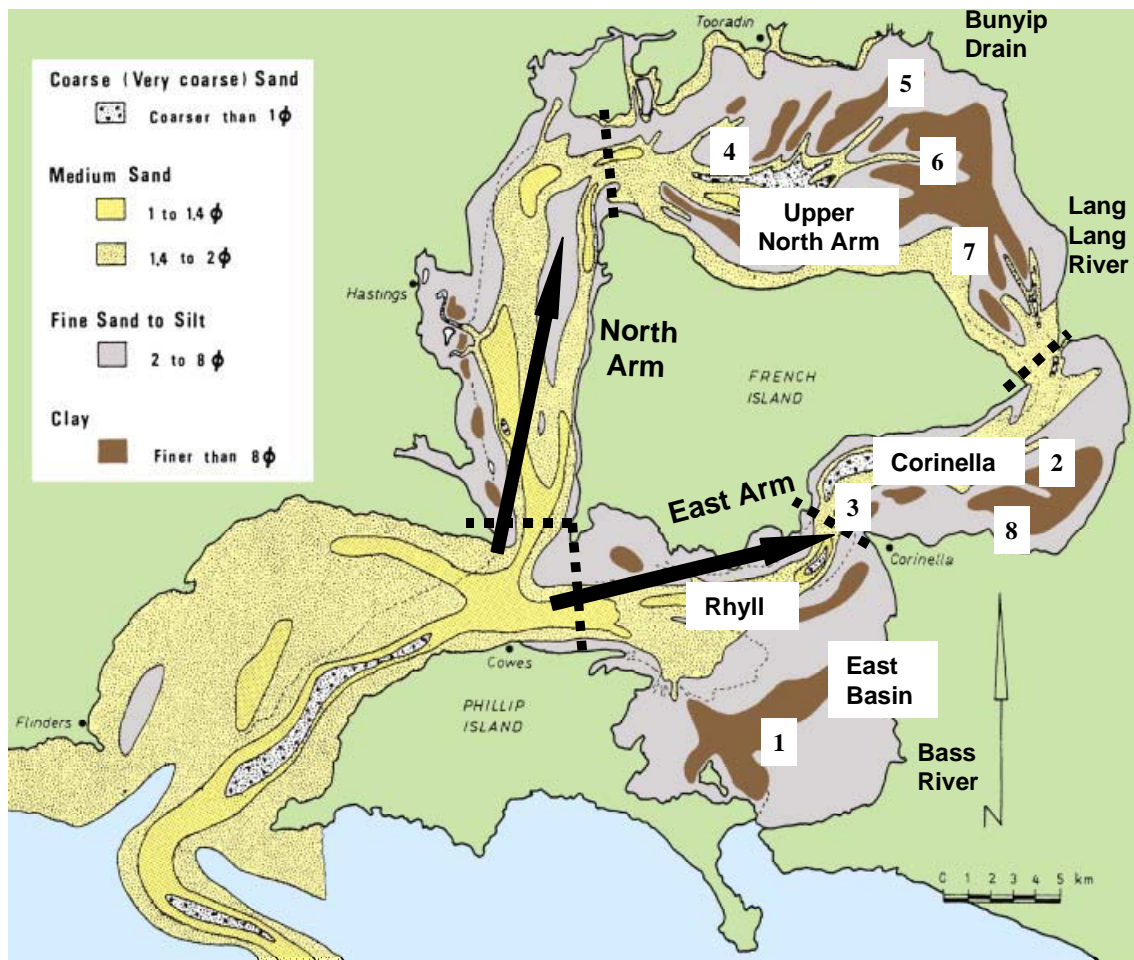


**Fig. 1. Sediment grain size distribution in Western Port (from Marsden et al., 1979). Segments and sample collection sites are shown. Segments are separated by dotted lines.**

**Table 1. Sample collection information**

Site	Coordinates	Approx. location	Water depth	Water samples	Cores (diameter)	Core length (cm)
1	S 38° 29.059 E 145° 22.897	East Basin; in mud lens adjacent to mouth of Bass River	5 m	Ebb tide 580 litres	2 x 100 mm 1 x 50 mm	40, 43 135
8	S 38° 23.923 E 145° 29.619	Corinella segment near Temby Point	3 m	Flood tide 780 litres	1 x 100 mm	69
2	S 38° 22.384 E 145° 30.900	Corinella segment: midway between Corinella and Jan Jerup point	2 m	Ebb tide 450 litres	2 x 100 mm 1 x 50 mm	43, 46 160
3	S 38° 23.433 E 145° 25.138	Main channel near Corinella	11 m	Flood tide 680 litres	No cores taken	
7	S 38° 17.422 E 145° 28.197	NE Bay; adjacent to mouth of Lang Lang River	1.5 m	Ebb tide 535 litres	1 x 100 mm 1 x 100 mm	36 77
6	S 38° 14.873 E 145° 27.526	NE Bay; adjacent to mouth of Yallock Ck	2 m	Ebb tide 755 litres	1 x 100 mm 1 x 50 mm	40 51
5	S 38° 14.008 E 145° 27.306	NE Bay; adjacent to mouth of Bunyip Drain	2 m	No water collected	2 x 100 mm	47
4	S 38° 15.234 E 145° 21.683	North Bay: near Charing Cross Channel	2 m	Flood tide 675 litres	2 x 100 mm	22, 22
4	S 38° 15.087 E 145° 21.563	North Bay: near Charing Cross Channel	4.5 m	Ebb tide 690 litres	1 x 100 mm	55

Collection of surface sediment samples for particle size analysis occurred over a period of 6 days in September 2001. The sediment samples were collected using an 'Eckman' grab sampler. This device captures up to 300 g of bottom sediment to a depth of ~10-15cm over an area of ~300 cm<sup>2</sup>. Sampling sites were selected using a grid based procedure (Fig. 2), and located by GPS on the VicEPA vessel. In total 148 samples were taken.

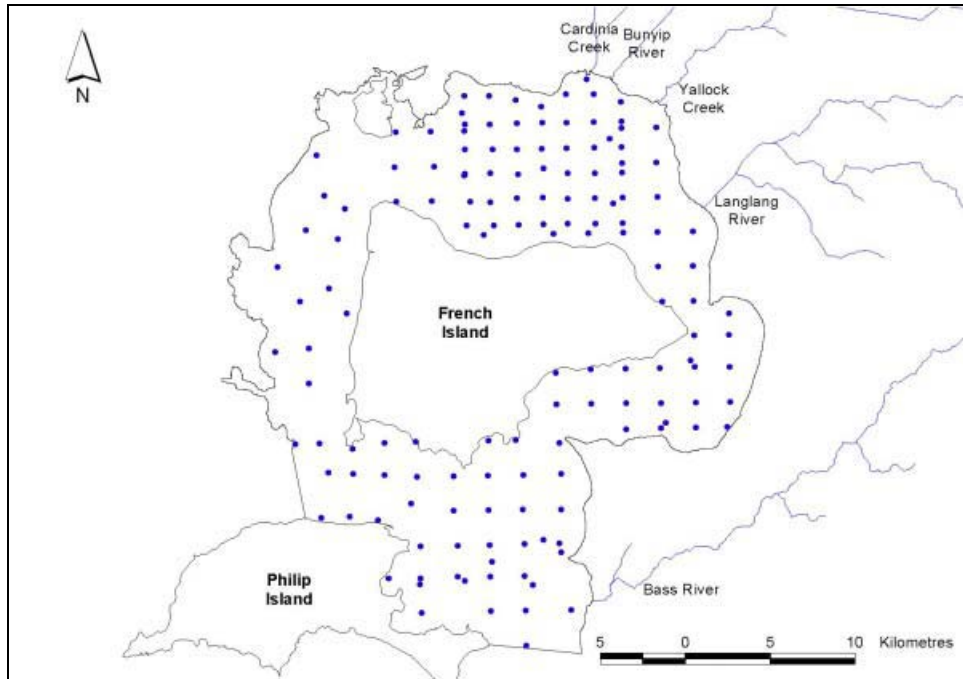


**Fig. 2. Locations of sediment grab samples for particle size determination.**

## 2.2 Analytical procedures

### *Sediment cores*

Visual descriptions of all cores were made prior to analysis, and are listed in Table 2. Descriptions of PVC cores were made after splitting the core in half lengthwise. Eight cores were sectioned for analysis.

The cores were partially thawed in the laboratory and sectioned into depth intervals ranging from 1 cm to 6 cm. Near-surface sections were sampled at smaller depth intervals. Water content (for porosity) and dry mass was determined for each section. Sediment dry density was also determined.

All sediment core sections were sieved prior to further analysis. The sediment was partitioned into particle size fractions;  $>500\ \mu\text{m}$ ,  $500\text{--}63\ \mu\text{m}$  and  $<63\ \mu\text{m}$ . All size fractions were dried and weighed. The  $>500\ \mu\text{m}$  fraction was not used for further analysis. The  $>63\ \mu\text{m}$  fraction was sub-sampled for XRF analysis; the two fractions  $<500\ \mu\text{m}$  were recombined in their original proportions for alpha and gamma spectrometry (see below).

The total sediment fraction  $<500\ \mu\text{m}$  was analysed using high-resolution gamma spectrometry (Murray et al., 1987) for  $^{238}\text{U}$ ,  $^{226}\text{Ra}$ ,  $^{210}\text{Pb}$  and  $^{137}\text{Cs}$ . Sediment was ashed at  $450^\circ\text{C}$  for 16 hours to determine loss on ignition (LOI). It was then cast in resin and counted for 1-2 days using intrinsic germanium gamma detectors. The detectors were calibrated using CANMET uranium ore BL-5, and thorium nitrate refined in 1906 (Amersham International).

Radiochemical separation and alpha spectrometry (Martin and Hancock, 1992) was used to give improved estimates of  $^{210}\text{Pb}$  in selected samples (via  $^{210}\text{Po}$  analysis). This method involves the addition of a tracer isotope of known activity (supplied by Amersham,  $\pm 1\%$  uncertainty), followed by radiochemical separation and electroplating. The electroplated discs were counted using high-resolution alpha spectrometry.

Major and trace element concentrations were determined on the  $<63\ \mu\text{m}$  fraction of sediment using XRF analysis. Prior to analysis the sediment was washed free of interstitial salt by shaking the sediment with demineralised water, centrifuging and decantation. This process was repeated until less than 1% of the original salt remained. Major elements were fused in a lithium borate matrix (Norrish and Hutton, 1969). Trace elements were determined using the pressed powder method (Norrish and Chappell, 1977).

### *Surface sediment samples*

After collection the sediment samples for particle size analysis were chilled and transported to the CSIRO laboratories in Canberra for size analysis. Samples were initially sieved to remove sediment  $>2\ \text{mm}$ . This mostly removed shell fragments. Smaller shell fragments and fine carbonates were removed by 10% HCL. Organic material was decomposed using 10% hydrogen peroxide. Sodium hexametaphosphate (Calgon) was added to the treated sample as a dispersant, and sieving and settling techniques were used to separate the particle size classes. The sediment pretreatment and separation procedures are given as a flowchart in Fig. 3. Size classes are  $<4\ \mu\text{m}$  (clay minerals),  $4\text{-}63\ \mu\text{m}$ ,  $63\text{-}125\ \mu\text{m}$ ,  $250\text{-}125\ \mu\text{m}$ ,  $250\text{-}500\ \mu\text{m}$  and  $>500\ \mu\text{m}$  (coarse sands).

The size class data were entered into ARCVIEW and a surface fitting algorithm used to fit isolines of percent mass for each size class. These were then presented as a series of overlays. All sediment masses are expressed the dry weight of mineral (inorganic) material, and collated as percentage mass by size class at each location.

Table 2. Core descriptions

Site	Location	Description
1	East Arm, East Basin, 135 cm depth	0-16 cm; dark fine-grained clay-rich mud 16-24 cm; clay-rich mud with small shell fragments 24-42 cm; clay-rich mud with large shell fragments increasing with depth; many intact mollusc shells. 42-135 cm; base of shell bed at 42 cm. Clay-rich mud below 42 cm with no visible stratification
8	East Arm, southern Corinella segment 69 cm depth	0-20 cm; brownish fine-grained clay-rich mud; some cavities indication the presence of fauna 20-42 cm; dark clay-rich mud with large shell fragments 42-60 cm; dark clay-rich mud; occasional small shell fragments 60-69 cm; dark clay-rich mud; occasional large shell fragments
2	East Arm, North Corinella segment 160 cm depth	0-30 cm; dark clay/silt/sandy sediment; no visible stratification 0-50 cm; as above, increasing sand content 50-70 cm; increasing density of large shell fragments with depth 50-160 cm; base of shell bed at 70 cm; dark clay-rich mud; decreasing water content with depth.
7	Upper North Arm inter-tidal; Near mouth of Lang Lang R. 36 cm depth	0-8 cm; brownish clay/silt/sand 8-20 cm; brownish clay/silt/sand with large shell fragments; isolated spherical patches of dark organic-rich sediment, 1-2 cm in diameter. 20-30 cm; less shell fragments; increasing content of dark organic rich material. 30-36 cm: dark brown fibrous peaty organic matter dominant
6	Upper North Arm inter-tidal; near mouth of Yallock Ck 51 cm depth	0-12 cm; brownish clay/silt/sand 12-22 cm; brownish clay/silt/sand; large shell fragments 28-51 cm; compact dark brown clay; low water content; occasional coarse angular gravel-sized fragments of terrestrial origin
5	Upper North Arm inter-tidal Near mouth of Bunyip Drain 48 cm depth	0-10 cm; sandy with small intact shells 10-20 cm; sandy with large shell fragments; black patches of sediment, possibly organic-rich, 1-2 cm in diameter; occasional plant filaments 2-3 cm in length 20-32 cm; increasing density of large shell fragments; numerous intact bivalves; patches of dark sediment 32-48 cm; decreasing shell fragments and increasing clay and silt content
4	North Arm: near Charing Cross Channel 69 cm depth	0-15 cm; dark brown clay/silt/sand 15-40 cm; large shell fragments increasing in density with depth; intact valves. 40-70 cm; dark clay/silt/sand; increasing mud content.

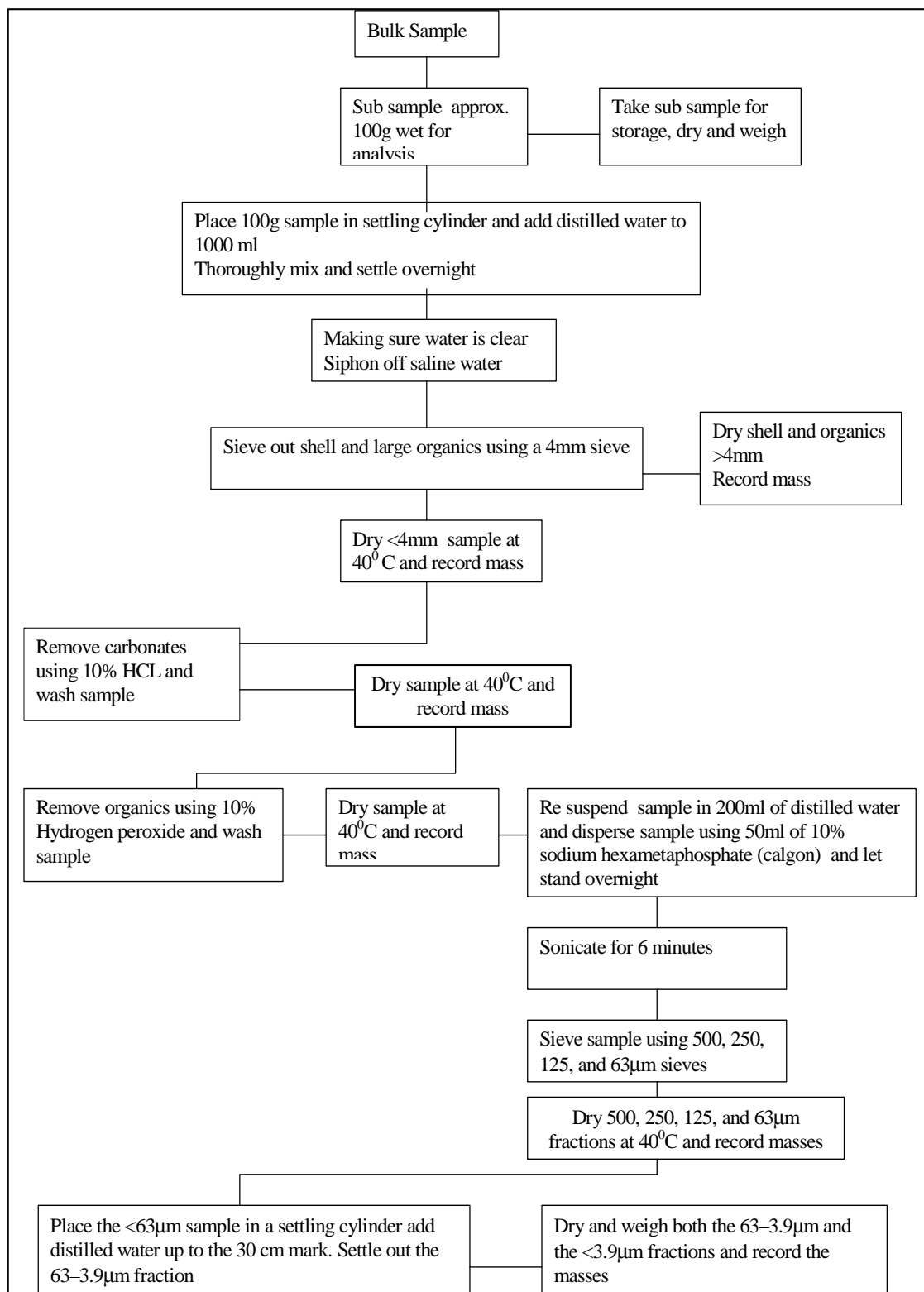


Fig. 3. Sample analysis procedure for particle size determination

### *Water samples*

Filter cartridges were ashed at 450° C and analysed for <sup>234</sup>Th by gamma spectrometry. Suspended sediment concentrations were determined by filtration of the water sample through a 0.2 µm membrane filter, and determination of the dry mass retained by the filter.

### **2.3 Tracers and chronometers**

The sources and pathways of the radionuclide tracers used in this study are illustrated in Fig. 4.

#### *Suspended particle residence time*

Suspended particle residence times are estimated from the activity of ‘excess’ <sup>234</sup>Th accumulated by particles in the water column. The method utilises the fact that dissolved <sup>234</sup>Th (half-life 24 days) is produced by decay of <sup>238</sup>U dissolved in sea water. Being particle-reactive, dissolved Th is rapidly scavenged by suspended particles. The amount of <sup>234</sup>Th activity scavenged by particles is related to the amount of time a particle has spent suspended in sea water. The scavenged <sup>234</sup>Th is removed from the water column by particle deposition, advection to Bass Strait and radioactive decay.

#### *Sediment accumulation and chronology using excess <sup>210</sup>Pb and <sup>137</sup>Cs*

The two fallout chronometers used in this study are ‘excess’ <sup>210</sup>Pb, and <sup>137</sup>Cs. Both these radionuclides accumulate in soils and sediments as a result of atmospheric fallout. Radioactive <sup>210</sup>Pb (half-life 22 years) occurs throughout nature, but the “excess” component found in sediments is usually generated in the atmosphere by decay of radioactive radon gas. Once formed, atmospheric <sup>210</sup>Pb rapidly attaches itself to dust particles, and is deposited as dry dust or with rainfall. Fallout <sup>210</sup>Pb leads to the accumulation of <sup>210</sup>Pb activity over and above that already present in the sediment. The additional <sup>210</sup>Pb is termed ‘excess’ <sup>210</sup>Pb, and is determined by the difference between the total <sup>210</sup>Pb and <sup>226</sup>Ra activities of the sediment. Once isolated by burial, the excess <sup>210</sup>Pb activity of sediment decreases by radioactive decay. Under favourable conditions the rate of sediment accumulation can be determined by the distribution of excess <sup>210</sup>Pb in the sediment profile (Appleby and Oldfield, 1992). The most commonly used model for the determination of sediment chronologies is the Constant Rate of Supply (CRS) model. Using this model the age (*t*) of sediment at depth *i* is calculated from

$$t_i = -\frac{1}{\lambda} \ln \left[ \frac{A(i)}{A(\infty)} \right] \quad (1)$$

where *A(i)* is the integrated activity (Bq m<sup>-2</sup>) of excess <sup>210</sup>Pb below depth *i*, and *A(∞)* is the total integrated activity of the sediment column. The model has a set of assumptions, the validity of which depend on the mechanisms of sediment and <sup>210</sup>Pb delivery to the sediment accumulation zone of the water body.

Cs-137 (half-life 30 years) is an artificial “man-made” radionuclide originating from the atmospheric testing of nuclear weapons that began in the 1950s. The testing resulted in atmospheric fallout of  $^{137}\text{Cs}$  on a global scale, and it is detected in surface soils of all continents. Olley et al. (1990) calculated that the detection of  $^{137}\text{Cs}$  in Australian sediments indicates that the sediments were deposited after 1958 (assuming  $^{137}\text{Cs}$  had remained immobile in the sediment profile).

Excess  $^{210}\text{Pb}$  and  $^{137}\text{Cs}$  are measured using the alpha and gamma spectrometry procedures outlined above.

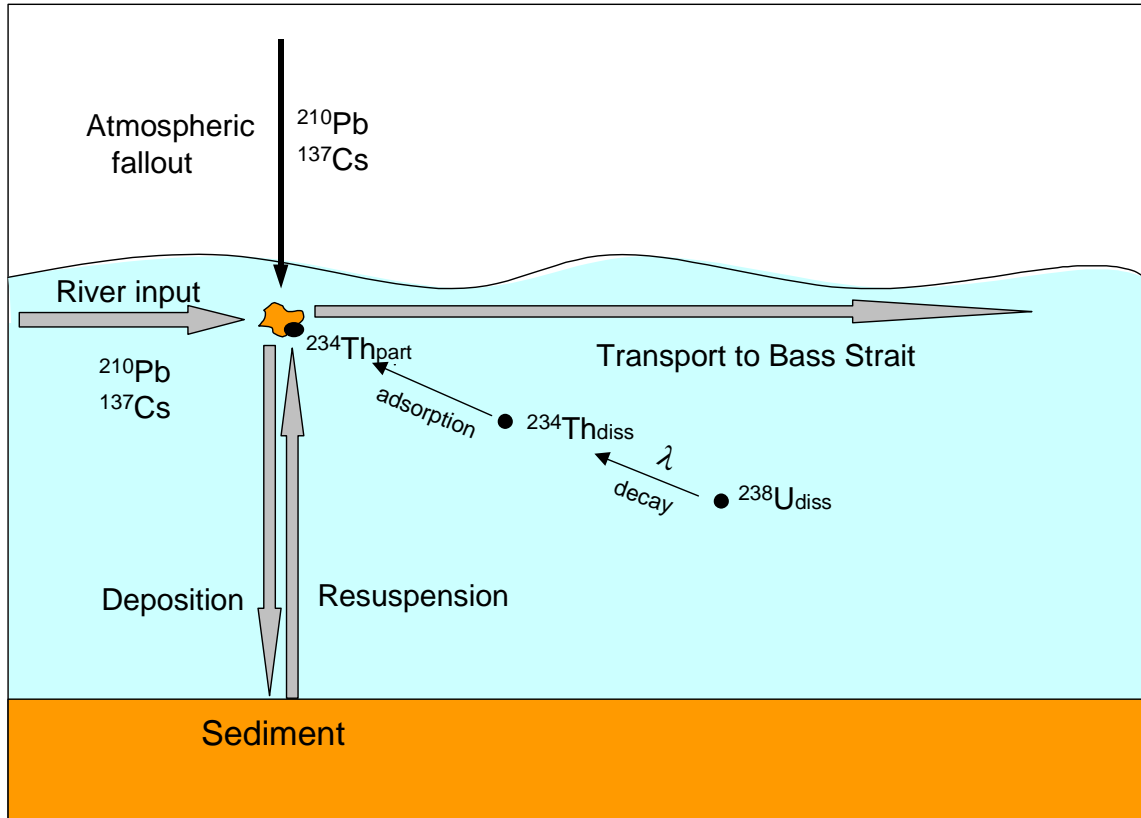


**Fig. 4. Schematic of radionuclide tracers and chronometers**

#### *Optically Stimulated Luminescence (OSL) dating*

Optical dating is used to estimate the time elapsed since buried sediment grains were last exposed to sunlight (Huntley et al., 1985; Aitken, 1998). The method uses the release of electrons from light-sensitive traps in the crystal defects of quartz and feldspar grains. On exposure to sunlight trapped electrons are released, resetting the OSL signal to zero. When the grains are buried and hidden from sunlight, they begin to accumulate a trapped-electron population due to the effect of ionizing radiation emitted by the decay of radionuclides present in the deposit. Some of this natural radioactivity may be derived from within the quartz or feldspar grains, but the radiation dose is mainly derived from the surrounding material. If the effective ionizing radiation is constant, then the burial time of the grains can be determined by

measuring the dose response stored in the grains (burial dose;  $D_e$ ), divided by the effective ionizing radiation (the dose rate;  $D_r$ ) such that

$$\text{Burial-time (years)} = \text{Burial-dose (Gy)} / \text{Dose Rate (Gy year}^{-1}\text{)} \quad (2)$$

Dating of sediment by OSL involves measurements of many discrete aliquots of sediment grains. These measurements yield an age distribution for each sample. The range of this distribution depends on how well the grains are bleached (how well the OSL signal is set to zero prior to deposition) and the extent of post-depositional mixing of sediment. The OSL age distribution of each sample needs to be considered with these factors in mind.

#### Preparation and analysis

Sediment samples were taken from the cores in the laboratory under subdued red illumination. Sand grains (180-212  $\mu\text{m}$  in diameter) were extracted by wet sieving and etched in hydrofluoric acid. Additional sub-samples of core material were taken adjacent to the OSL samples for determination of water content and lithogenic radionuclide concentrations.

The burial dose was determined by measurement of the OSL from small aliquots (1 mm diameter) of quartz grains. All measurements were made on a Risø automated TL/OSL reader, fitted with a photomultiplier tube and three U-340 transmission filters. The machine has a  $^{90}\text{Sr}/^{90}\text{Y}$  beta source. The aliquots were analysed using the regenerative-dose protocol described by Roberts et al. (1998), which was modified from those presented by Murray and Roberts (1998) and by Murray and Mejdahl (1998). The field dose rates were determined by laboratory analysis of the radionuclide concentration in the samples taken from adjacent to the OSL samples. The reported uncertainties of OSL dates are determined by propagating the uncertainties of field and reader doses.

#### *Pinus pollen*

Pine trees are exotic to Australia, and detection of *Pinus* pollen in sediment profiles can be used as a chronological marker. Pines were first introduced to Australia in late 1850's and were planted extensively in Victoria by 1870 (Fielding, 1957). The most common species, Monterey Pine (*Pinus radiata*) begins pollinating after 3-9 years of age. Large amounts of pollen are released and dispersed by individual trees annually, and grains of *Pinus* pollen in southern Australia were probably entering regional pollen rains by about 1880. Significant increases in the regional flux of pollen are likely to have occurred when plantations of Pines were established in Victoria around 1920. Although the timing of the first appearance of *Pinus* pollen in aquatic sediments undoubtedly varies between regions, it is probable that *Pinus* pollen was widespread in Victoria by the late 1800's (Ogden, 2000).

#### Preparation and analysis

The method is a modification of a Cladoceran extraction method (Ogden, 1996). A 1-2 mL sub-sample of sediment was dispersed in hot 10% KOH. To aid recognition, pollen grains were stained pink by addition of saffranin. The dispersed sediments were then sieved and the silt fraction (35-63  $\mu\text{m}$  particle size range), which included

*Pinus* grains, was isolated. *Pinus* grains were separated from silt-sized inorganic and coarse-silt organic particles by settling through a 120 cm glass column. *Pinus* grains remained in suspension, and were collected and concentrated to 2 mL in volume by sieving.

The whole sample was counted under a dissecting scope at 60x magnification. About 1/8 of the sample was removed at a time using a Pasteur pipette and smeared across a microscope slide, which was left uncovered for counting. Results are expressed as grains per mL wet sediment.

### 3. Sediment Transport and Distribution

#### 3.1 Suspended particle residence time

The particle residence time,  $\tau_p$ , is determined from the equation

$$\tau_p = \frac{1}{\lambda_{Th}} \left[ \frac{A_{Th}^p}{A_U^d - (A_{Th}^d + A_{Th}^p)} \right] \quad (3)$$

where

$A_{Th}^p$  is the excess particle-bound activity of  $^{234}\text{Th}$  ( $\text{Bq m}^{-3}$ ), given by the difference in the particle-bound activities of  $^{234}\text{Th}$  and  $^{238}\text{U}$ ;

$A_{Th}^d$  is the dissolved activity of  $^{234}\text{Th}$  ( $\text{Bq m}^{-3}$ );

$A_U^d$  is the dissolved  $^{238}\text{U}$  activity ( $\text{Bq m}^{-3}$ ),

and  $\lambda_{Th}$  is the  $^{234}\text{Th}$  decay constant ( $= \ln 2 / \text{half-life} = 0.029 \text{ day}^{-1}$ ).

Suspended particulate material (SPM) and dissolved activities of  $^{238}\text{U}$  and  $^{234}\text{Th}$  are given Table 3, along with calculated values of  $\tau_p$ . Dissolved  $^{238}\text{U}$  was measured in two samples, and found to be  $39 \text{ Bq m}^{-3}$ , a value close to that of the open ocean. At the time of sampling the salinity of Western Port did not vary significantly from the ocean value (around 36), and the dissolved  $^{238}\text{U}$  activity of bay water is likewise assumed constant. Most of the measured values of dissolved  $^{234}\text{Th}$  ( $A_{Th}^d$ ) are close to, or below detection, and the mean value of all measurements of  $A_{Th}^d$  ( $0.3 \text{ Bq m}^{-3}$ ) has been used in Eqn. 3. Although the relative uncertainty of  $A_{Th}^d$  is high, variation within its measured range ( $0\text{-}2 \text{ Bq m}^{-3}$ ) has very little effect on  $\tau_p$ .

In applying Eqn. 3 there are two main assumptions. First, steady state, on a time scale approaching the  $^{234}\text{Th}$  half-life, is assumed with regard to Th scavenging and removal. This assumption will not always hold in a dynamic environment like Western Port, the most significant parameter showing short-term variation being SPM. Nevertheless, the steady-state assumption can still serve as a useful starting for a comparison of various deposition environments within the bay. SPM concentrations at the time of this study were similar at all sites, and close to the concentration mean of data from longer-term monitoring sites (data from Victorian EPA). This observation indicates SPM fluctuations were not likely to have seriously affected determinations of  $\tau_p$  at the time of sampling.

The second assumption supposes that particles entering the water column of Western Port have zero excess  $^{234}\text{Th}$ . Major sources of SPM to the bay include particles with delivered river water, particles resuspended from the bay floor, and particles from Bass Strait. Due to the very low  $^{238}\text{U}$  activities in river water, riverine particles contain very little excess  $^{234}\text{Th}$ . Concentrations of particle-bound  $^{234}\text{Th}$  in the ocean are typically  $1\text{-}2\text{ Bq m}^{-3}$ , similar to values in Western Port water (Table 3). Depending on the rate of exchange of northern and eastern bay water with ocean water, input of oceanic particles may contribute significantly to the observed particle-bound activity of  $^{234}\text{Th}$  in Western Port, elevating our estimate of  $\tau_p$ . Particles deposited onto the floor of the bay will lose most of the excess  $^{234}\text{Th}$  that they accumulated while in the water column by radioactive decay over a period of weeks to months. However if the particle is resuspended within this time frame, some residual excess  $^{234}\text{Th}$  activity will remain from the previous resuspension event. This residual activity will lead to an overestimate of  $\tau_p$  for the new period of resuspension.

This assessment indicates that the values of  $\tau_p$  given in Table 3 may be too high. However all values of  $\tau_p$  are very low ( $<1.5$  days). On this time scale over-estimation of  $\tau_p$  has no bearing on our conclusion (section 3.4 below) relating to the mechanism of particle resuspension and transport.

**Table 3. Particle residence times calculated from  $^{234}\text{Th}$  and  $^{238}\text{U}$  data.**

Site	Location	SPM $\text{mg L}^{-1}$	Particulate $^{234}\text{Th}$ $\text{Bq kg}^{-1}$	Particulate $^{238}\text{U}$ $\text{Bq kg}^{-1}$	Particulate $^{234}\text{Th}_{\text{ex}}$ $\text{Bq kg}^{-1}$	Particulate $^{234}\text{Th}_{\text{ex}}$ $\text{Bq m}^{-3}$	Dissolved $^{234}\text{Th}$ $\text{Bq m}^{-3}$	$\tau_p$ (days)
1	East Basin	6.9	$135 \pm 13$	$13 \pm 9$	$123 \pm 21$	$0.85 \pm 0.15$	$0.1 \pm 0.0$	$0.77 \pm 0.13$
8	Corinella South	8.4	$163 \pm 21$	$21 \pm 7$	$142 \pm 16$	$1.19 \pm 0.13$	$0.3 \pm 0.1$	$1.09 \pm 0.12$
2	Corinella North	10.0	$78 \pm 15$	$12 \pm 8$	$66 \pm 20$	$0.66 \pm 0.20$	$0.5 \pm 1.4$	$0.60 \pm 0.18$
3	East Arm Channel	7.1	$236 \pm 26$	$20 \pm 10$	$216 \pm 31$	$1.53 \pm 0.22$	$0.3 \pm 0.5$	$1.42 \pm 0.21$
4	Charing Cross (ebb)	7.6	$121 \pm 13$	$8 \pm 7$	$113 \pm 17$	$0.86 \pm 0.13$	$0.2 \pm 0.2$	$0.78 \pm 0.12$
4	Charing Cross (flood)	8.9	$135 \pm 13$	$18 \pm 6$	$117 \pm 15$	$1.04 \pm 0.14$	$0.3 \pm 0.7$	$0.95 \pm 0.12$
6	Yallock Ck.	7.6	$122 \pm 13$	$9 \pm 6$	$113 \pm 17$	$0.86 \pm 0.13$	$0.3 \pm 1.9$	$0.78 \pm 0.12$
7	Lang Lang	7.9	$135 \pm 14$	$15 \pm 9$	$121 \pm 18$	$0.95 \pm 0.14$	$0.2 \pm 0.1$	$0.87 \pm 0.13$

The distribution of  $\tau_p$  in Western Port is shown in Fig. 5. No spatial trend is seen, with most values lying between 0.6-1.0 day. These small values indicate a dynamic cycle of frequent input and rapid removal of particles from the water column. The implications for particle transport in the bay are discussed in section 3.4 below.

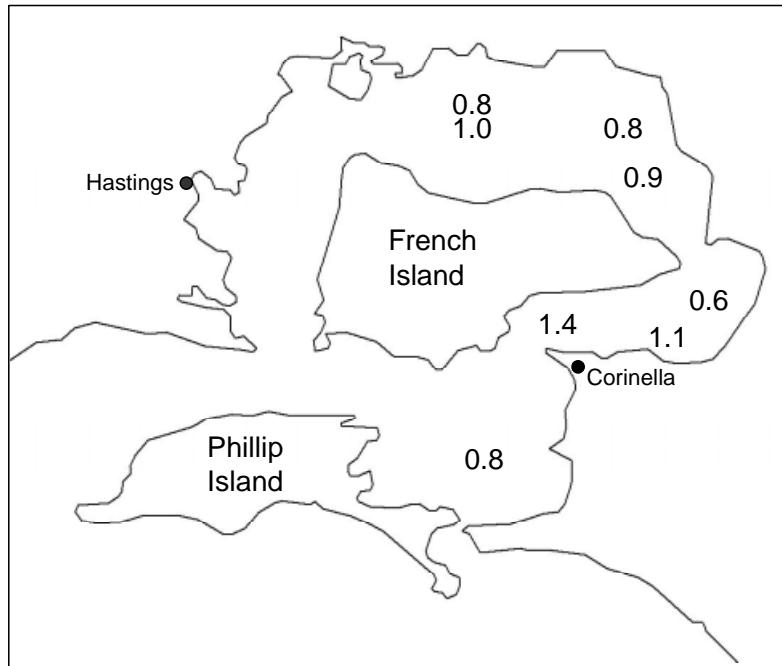


**Fig. 5. Distribution of suspended particle residence times ( $\tau_p$ ). Units are days.**

### 3.2 Sediment distribution

The distribution of the particle size fractions are shown in Fig. 6. The distribution of clay-rich sediment ( $<4 \mu\text{m}$ ) appears to be consolidated within three main regions of the bay; the eastern side of the Upper North Arm in a zone extending  $\sim 5 \text{ km}$  offshore encompassing the mouths of Yallock Creek and the Lang Lang River; the eastern edge of the Corinella segment (two main areas); and the Rhyll segment including the East Basin. Some of these regions match the distribution of the corresponding size fraction mapped by Marsden et al., (1979) (Fig. 1), although there are two major differences. The first is that clay deposits mapped by Marsden offshore from the Bunyip Drain and Cardinia Creek are no longer present. The second major difference is the appearance of major clay-rich deposits offshore of eastern Phillip Island, adjacent to the East Basin.

The ‘mud’ ( $<63 \mu\text{m}$ ) class of sediment includes, clay, silt and fine sands. Its distribution shows a similar pattern to the clay fraction, with the same three zones of accumulation. The sediment size fractions  $>63 \mu\text{m}$  (light areas) are concentrated in the deeper channels and adjacent to the mouths of Cardinia Creek, Bunyip Drain and Bass River.

The coarsest size fraction ( $>500 \mu\text{m}$ ) is present in the lobes offshore of the Cardinia and Bunyip, but not the Bass. Sediment adjacent to the Bass River mouth falls mainly in the  $250\text{-}500 \mu\text{m}$  size range. Only minor deposits of fine sands are seen off-shore from the Lang Lang River mouth.

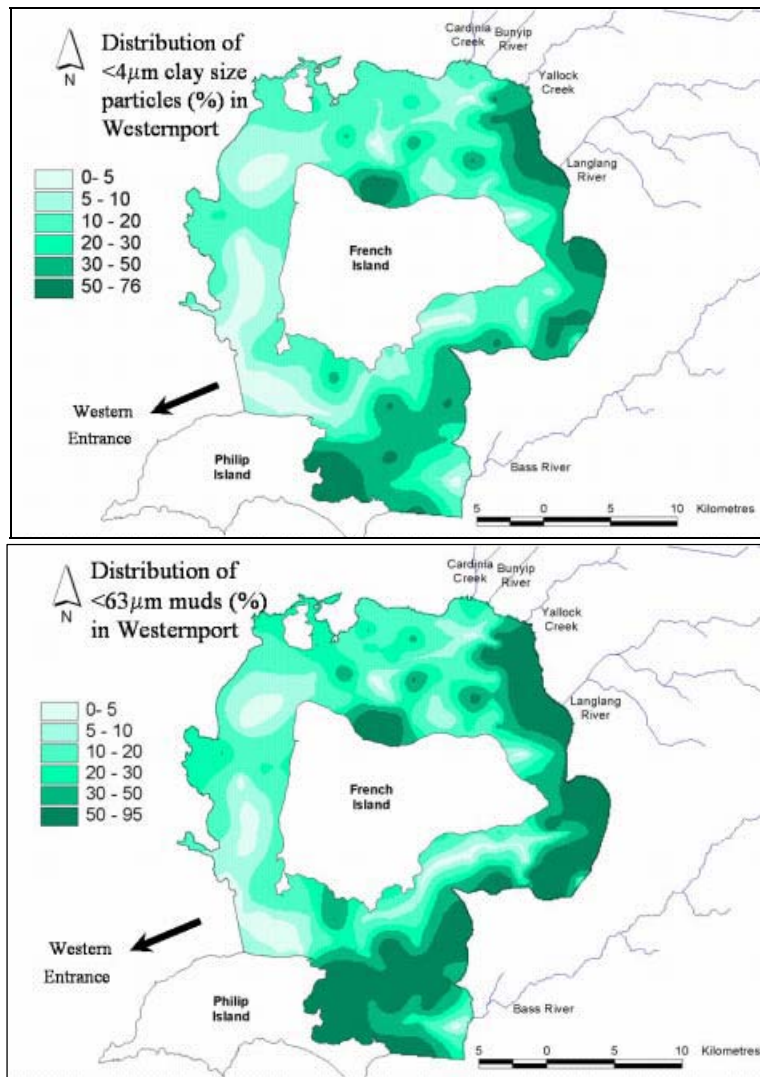


**Fig. 6. Particle size distribution (%) of surface sediment;  $<4\mu\text{m}$  (top) and  $<63\mu\text{m}$  (bottom).**

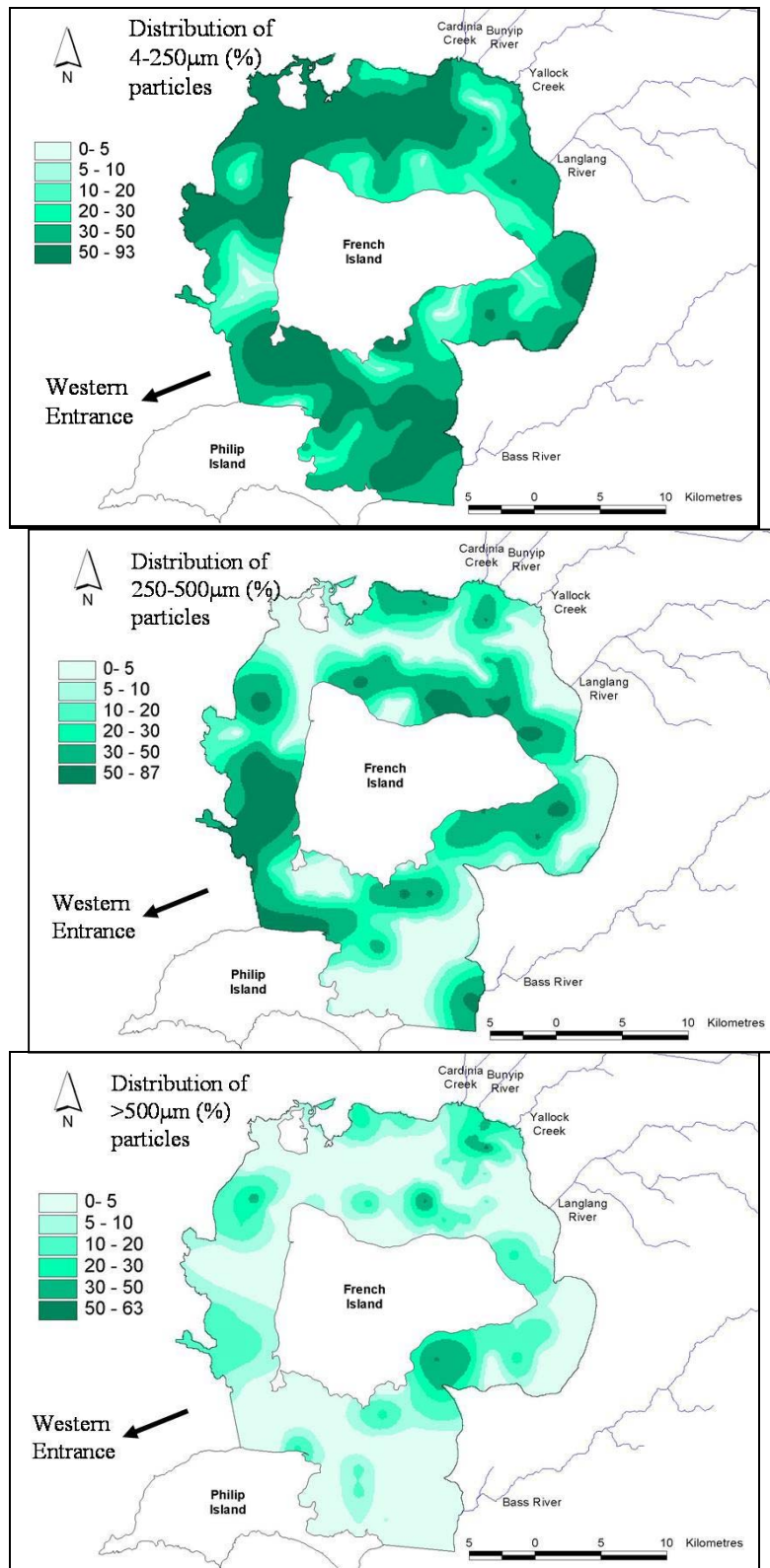


**Fig. 6. continued. Particle size distribution of surface sediment; 4-250 µm (top); 250-500 µm (middle) and >500 µm (bottom).**

### 3.3 Excess $^{210}\text{Pb}$ and $^{137}\text{Cs}$ inventories

Bottom sediment inventories of excess  $^{210}\text{Pb}$  and  $^{137}\text{Cs}$  activity are determined by integrating their activities over the entire sediment profile, from the surface down to a level where the excess  $^{210}\text{Pb}$  activity is consistent with zero, ie.

$$I = \sum_{i=1}^{\infty} A_i \quad (4)$$

where  $A_i$  is the activity of the  $i^{\text{th}}$  section of the core, numbered downwards.

Analysis of the various particle size fraction of selected sediment grab samples from within the bay show that excess  $^{210}\text{Pb}$  and  $^{137}\text{Cs}$  is held almost exclusively held by the mud (<63  $\mu\text{m}$ ) fraction. Bottom sediment inventories of excess  $^{210}\text{Pb}$  and  $^{137}\text{Cs}$  are therefore expected to provide similar information to the <63  $\mu\text{m}$  sediment distribution map, but with the addition of time-averaged estimates of mud accumulation. By examining the values of inventories in various parts of the bay the relative efficiency of mud entrapment within specific zones over the last 40-60 years is quantified, indicating focal points for sediment deposition and longer-term transport routes.

The distribution of excess  $^{210}\text{Pb}$  and  $^{137}\text{Cs}$  inventories determined in seven cores is shown in Fig. 7. Inventories of both tracers are lowest in the Upper North Arm, and generally increase in a clockwise direction southwards. An exception is northern Corinella site (site 2), at which the  $^{137}\text{Cs}$  inventory in particular is much higher than all other sites. Explanations for this high value are discussed in section 4.2 below.

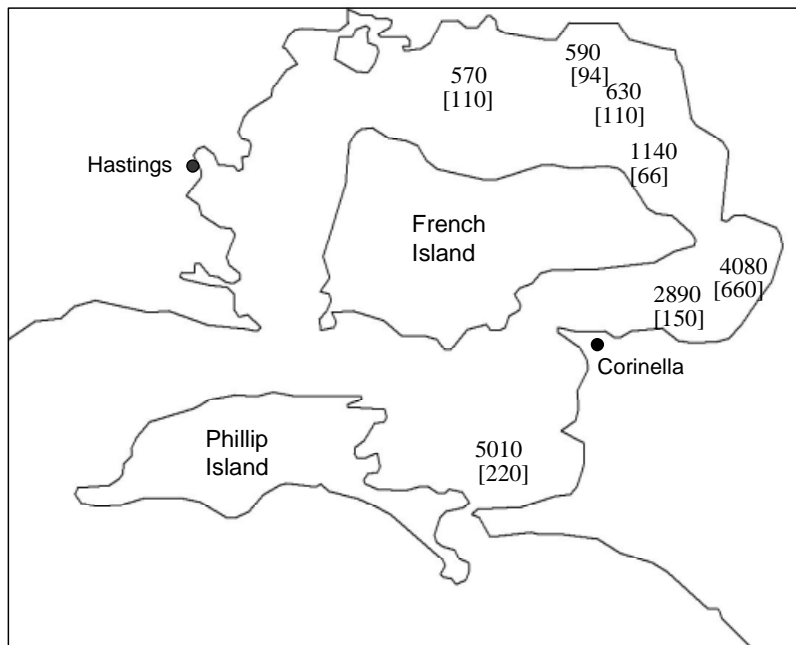


Fig. 7. Inventories of excess  $^{210}\text{Pb}$  and  $^{137}\text{Cs}$  (square brackets).

The excess  $^{210}\text{Pb}$  inventories in the Upper North Arm are much lower than the inventories expected solely from atmospheric fallout in southeast Australia. The expected excess  $^{210}\text{Pb}$  inventory due to fallout is  $2000 \text{ Bq m}^{-2}$  (Turekian et al., 1977). Normally low inventories would indicate a zone of low mud sedimentation and/or erosion of mud-sized sediment. East Arm sites show excess  $^{210}\text{Pb}$  inventories higher than expected from fallout, indicating that the Corinella and Rhyll segments are major deposition zones for mud.

### 3.4 Discussion and summary of sediment transport and distribution results

Suspended particle residence times of less than one day indicate a dynamic cycle of input and removal of suspended particles. The immediate source of the suspended particles to the water column is mainly resuspended sediment from the bay floor, rather than riverine sediment directly transported from the mouths of rivers and streams. This conclusion is reached via a simple mass balance calculation. The rate of removal of sediment from the bay water column ( $F$ ) can be roughly estimated by

$$F = C_p V \tau_p \quad (5)$$

where  $C_p$  is the mean SPM concentration in the bay ( $0.008 \text{ g L}^{-1}$ ), and  $V$  is the volume of water in the bay (about  $2 \times 10^9 \text{ m}^3$ ; Shapiro, 1975). A particle residence time of 1 day is used for  $\tau_p$ . Using these values  $F$  is estimated to be about  $6 \times 10^6 \text{ t yr}^{-1}$ , a load two orders of magnitude higher than sediment input loads estimated from river monitoring (section 1). Although terrestrial sediment undoubtedly makes up a large component of SPM in the bay, this calculation shows that the immediate source of the most of the SPM in the bay is not SPM delivered directly to the bay by rivers, but rather deposited sediment resuspended from the floor of the bay. This situation is only likely to change during rare periods of very high river flow.

The resuspension of sediment and its removal from the water column on a time scale of  $>1$  day is best explained by the action of the tides. Water movement in the bay is dominated by the motion of the tides (Marsden, 1979), and the potential exists for resuspension of sediment from the shallow inter-tidal regions of the Upper North Arm (Harris et al. 1979). The mechanisms of particle removal from the water column include redeposition onto the bay floor, and/or transport to Bass Strait. Of these two particle removal processes it is likely that deposition dominates. This is concluded from the very low and relatively constant values of  $\tau_p$  seen throughout the bay, and the trend in excess  $^{210}\text{Pb}$  and  $^{137}\text{Cs}$  inventories. Harris and Robinson (1979) indicated an exchange period of weeks-months for water in the upper parts of Western Port. If a significant fraction of suspended particles were being transported to Bass Strait during a single phase of suspension (ie. without being redeposited somewhere in the bay), a range of values of  $\tau_p$  (from days to weeks) would be expected, with values increasing southwards. To explain the short and relatively constant values of  $\tau_p$ , sediment transport must be happening mainly as a series of short ( $<1$  day) resuspension and deposition episodes, rather than as a single episode of resuspension and transport.

The deposition-resuspension cycle, in conjunction with the net clockwise movement of water in the bay (Marsden, 1979; Hinwood, 1979) provides a mechanism for sediment movement which is consistent with both the observed distribution of mud in the bay and the trend in excess  $^{210}\text{Pb}$  and  $^{137}\text{Cs}$  inventories. Fig 8 schematically describes the model of sediment transport and deposition which has emerged from this study, whereby fine-grained sediment is apparently being focussed in the eastern and southern regions of the bay by a continual cycle of resuspension and deposition. Some of the sediment deposited in the East Basin will certainly have been delivered through the mouth of the adjacent Bass River, but this model of sediment transport suggests a significant contribution from northern river inputs as well.

The model also provides a mechanism to explain the differences observed in the clay mineral distribution shown by the maps produced by Marsden et al. (1979) (Fig. 1) and our recent work (Fig 4). These differences indicate a decrease in the extent of mud-dominated areas in the north, and an increase in the south, especially in and around the East Basin. If these differences are a true reflection of changes in the sediment distribution, north-south transport of mud may have significantly changed the composition of the bottom sediment substrate in some areas of the bay over the last twenty years. Some of these apparent changes in substrate composition have occurred in areas affected by seagrass loss.

## **4. Sediment Accumulation**

### **4.1 Grain size composition of sediment cores**

Visual inspection indicated very little fine layering, although coarse bands of varying composition are present in all cores. The core from site 7 (Lang Lang) is unique, in that it contains what appears to be a thick layer of fibrous peat-like organic-rich material at depths greater than 25 cm. At site 8 (south Corinella) a distinct colouration change occurs at a depth of about 25 cm depth, from light brown to a dark grey. This change is not associated with organic matter content, and probably indicates a change from oxygen-rich to anaerobic conditions in the sediment. Bioturbation (mixing) in the upper sediment layer is probably responsible for this change.

Porosity varies from core to core, and is usually highest in the surface layer, and in layers of fine-grained clay-rich sediment. The organic matter content, as estimated by loss on ignition at  $450^\circ\text{C}$ , is mostly less than 15% by mass, the exception being site 7. This is probably related to the peat-like material (discussed above). Patches of dark sediment, possibly organic-rich, were seen below 10 cm in the core from site 5 (Bunyip Drain) but no trend is seen in the LOI data. Notably absent were recognisable remains of past seagrass beds in Upper North Arm cores, as noted by Wilk et al. (1979).

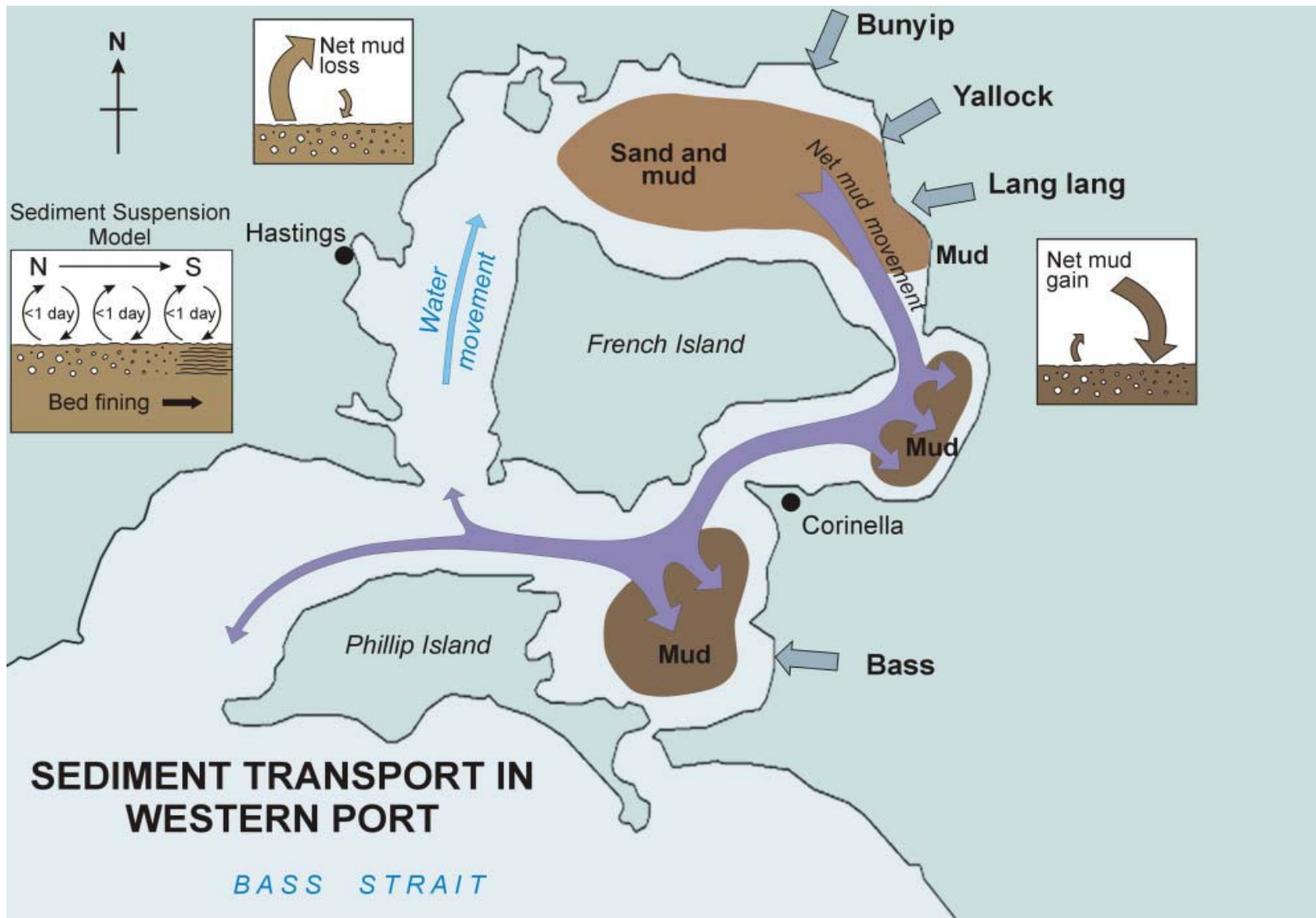


Fig. 8. Schematic illustrating the sediment transport model.

Three particle size fractions are used to broadly describe the composition of the sediment; >500  $\mu\text{m}$ , 500-63  $\mu\text{m}$ , and <63  $\mu\text{m}$ . In all cores except one the >500  $\mu\text{m}$  fraction is made up entirely of shell fragments, and this fraction has been used to estimate the shell content of the sediment. Once again the exception is the deep sediment from site 7 which contains fibrous matted organic matter. The degree of fragmentation of the >500  $\mu\text{m}$  fraction varies considerably, ranging from fully intact bi-valves up to 20 cm wide, to angular broken fragments not much greater than 500  $\mu\text{m}$ . The intermediate size fraction (500 to 63  $\mu\text{m}$ ) consists mostly of quartz grains, and this size fraction has been used to estimate the sand content of the cores. The finest size fraction (<63  $\mu\text{m}$ ) contains mostly silt and clay minerals.

Variations in the mud (silt/clay), sand and shell composition with depth in all seven cores are shown in Fig. 9. The LOI (organic) component is not included, so these figures represent just the inorganic (mineral) fraction of the sediment. All cores contain mud, but the content varies. The mud fraction is lowest in the surface 10 cm of the Upper North Arm, mostly lying in the range 8-40%, and greatest (>99%) in the cores from the south Corinella and East Basin sites. By contrast, the sand content of the cores is greatest at the northern sites, comprising 40-80% by mass in the upper 10 cm of sediment. In most of the northern cores the sand content increases towards the surface.

The shell content of the cores is also variable. Shell beds, made up of layers of intact and fragmented mollusc shells interspersed with sediment, are a feature of the East Arm cores. The beds generally cover a depth interval of about 20 cm. Upper North Arm cores also have a large component of shell fragments, but these fragments are more evenly distributed through the upper layer.

## 4.2 Application of chronological methods

Sediment accumulation was initially assessed using routine  $^{210}\text{Pb}$  and  $^{137}\text{Cs}$  geochronology. However doubts about the validity of the basic assumptions of this method, and the possibility of post-depositional mixing of the sediment profile has precluded high-resolution dating, and limited the time span over which dating could be confidently applied. Where suitable core sediment remained additional dating was undertaken using OSL and *Pinus* pollen methods. This was done to extend the historical period, and to corroborate  $^{210}\text{Pb}$  and  $^{137}\text{Cs}$  chronologies. Profiles of selected parameters from each site are shown in Figs 10-16. All sediment data is listed in the Appendix.

### *$^{210}\text{Pb}$ and $^{137}\text{Cs}$ geochronology*

In most cores excess  $^{210}\text{Pb}$  activity is highest near the top of the core, and decreases with depth. The depth at which excess  $^{210}\text{Pb}$  becomes undetectable varies from core to core (detection limit  $\sim 2\text{-}3 \text{ Bq kg}^{-1}$ ), but the depth of penetration of detectable excess  $^{210}\text{Pb}$  and  $^{137}\text{Cs}$  is greatest in the cores from the East Arm. These cores also show approximately constant excess  $^{210}\text{Pb}$  activity in the upper sediment layer.

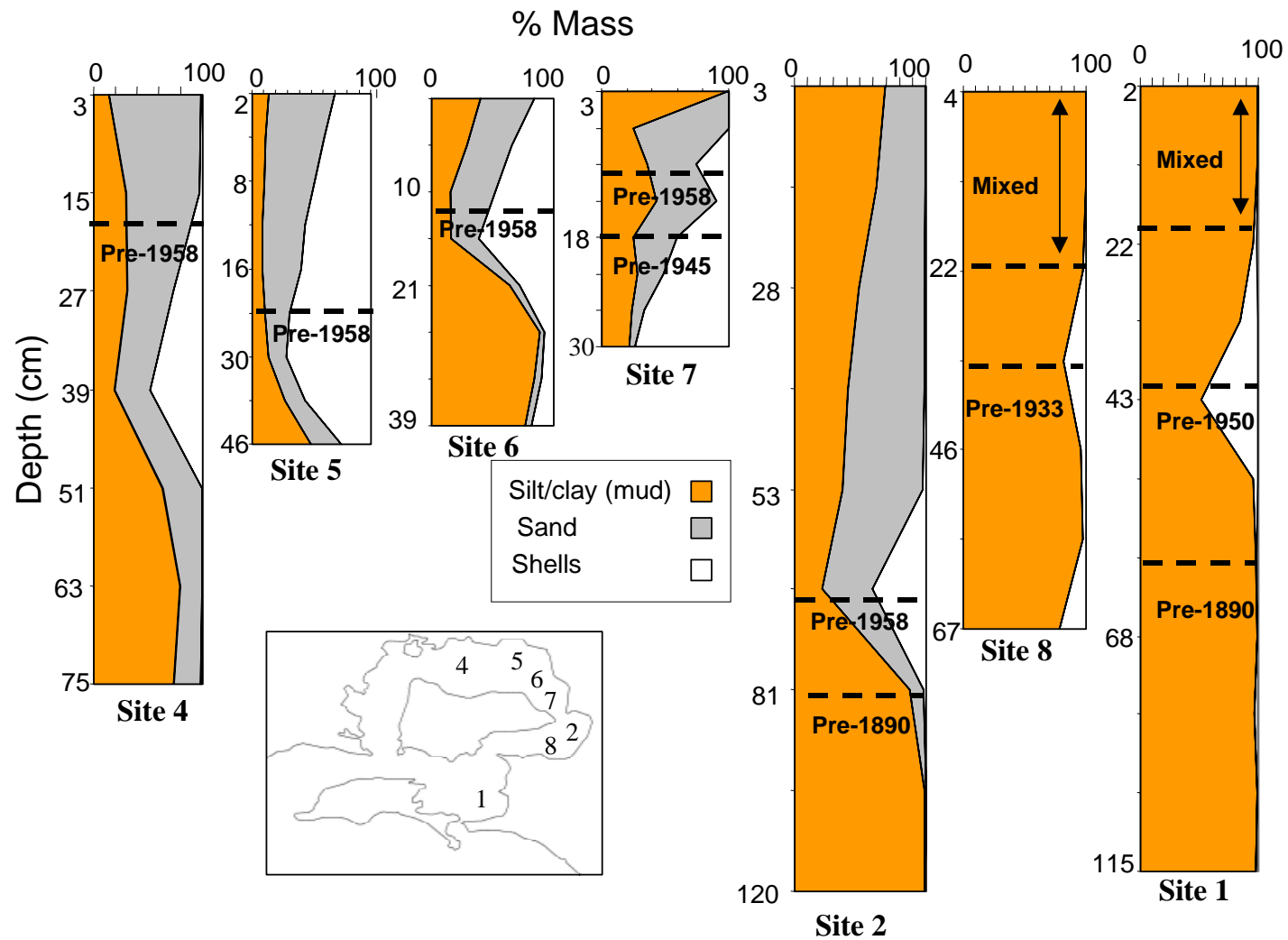


**Fig. 9. Sediment composition depth profiles. The organic (LOI) component has been excluded. Profiles listed from left to right correspond to a north-south clockwise direction around the bay (see inset)**

Mixing of the upper sediment layer by macrofauna (bioturbation) is common in marine sediment, and where it occurs on a time scale less than the  $^{210}\text{Pb}$  half-life (22 years) a layer of constant excess  $^{210}\text{Pb}$  activity is usually seen (eg. Hancock et al., 2000). In such cases a 2-layer mixing model (Berger and Heath, 1968) is sometimes applied to interpret the  $^{210}\text{Pb}$  profile. This model assumes vertical mixing of sediment occurs in an upper layer of constant depth at a more or less constant rate. Below the upper layer mixing is assumed absent. As sediment accumulates the mixed layer is assumed to move upwards in synchrony with the sediment column. As this happens sediment is transferred from the mixed layer into the unmixed layer at a rate determined by the rate of sediment accumulation. Once in the unmixed layer, excess  $^{210}\text{Pb}$  decays in accordance with its half-life. The mean rate of sediment accumulation averaged over the last 60-70 years (about three  $^{210}\text{Pb}$  half-lives) can be estimated from the slope of the linear regression of log excess  $^{210}\text{Pb}$  activity against depth in the segment of the profile immediately below the mixed layer (Figures 10, 11 and discussion below).

In applying the 2-layer model it is assumed that the excess  $^{210}\text{Pb}$  activity of the sediment transferred into the bottom (unmixed) layer is approximately constant. In most near-shore marine sediment this assumption is reasonable given the large apparent depth of the mixed layer (usually greater than 10 cm). Although the excess  $^{210}\text{Pb}$  activity of depositing sediment will vary as a result of the “flashy” nature of river flow and sediment delivery to the bay, the homogenising effect of bioturbation within a thick layer of sediment can have the effect of smoothing  $^{210}\text{Pb}$  activity variations to the point where steady  $^{210}\text{Pb}$  activity at the base of the mixed layer can be reasonably assumed. The other important assumption of the 2-layer model is that mixing is assumed absent below the mixed layer. If slow mixing is occurring below the rapidly mixed layer the rate of sediment accumulation will be over-estimated. Such a situation was seen in Port Phillip Bay sediment (Hancock and Hunter, 1999). Deep mixing may also occur in Western Port sediment, and accumulation rates determined using the 2-layer model should be considered upper limits.

In cores from the northern sites the excess  $^{210}\text{Pb}$  activity of the upper sediment is more variable, and interpretation more problematic. If mixing is occurring at these sites the depth and rate of mixing is uncertain, and application of the 2-layer mixing model is not viable. Proper application of the constant  $^{210}\text{Pb}$  flux model (the CRS model) is also questionable at some Upper North Arm sites, given the very few measurements of detectable excess  $^{210}\text{Pb}$  obtained from some core profiles, and the variable input of sediment (and hence  $^{210}\text{Pb}$ ) into this region of the bay. Nevertheless, a time horizon can often be determined by assessing  $^{210}\text{Pb}$  profiles in a similar way to  $^{137}\text{Cs}$ ; ie. by determining the depth at which excess  $^{210}\text{Pb}$  becomes undetectable. For most cores in the Upper North Arm excess  $^{210}\text{Pb}$  becomes undetectable at about 10-15% of the excess  $^{210}\text{Pb}$  activity of sediment at the surface of the core, equivalent to radioactive decay over a period of around three  $^{210}\text{Pb}$  half-lives (about 60 years). Using this rationale, it can be confidently predicted that the sediment horizon at which excess  $^{210}\text{Pb}$  becomes undetectable was deposited prior to 1940.

Figures 10-16. Sediment core profiles. Filled circles, excess  $^{210}\text{Pb}$ ; unfilled circles,  $^{137}\text{Cs}$ ; filled diamonds, mass ratio of P/Fe; unfilled diamonds, mass ratio of P/Al; unfilled squares, Cu; unfilled triangle, Mo; filled squares,  $\text{SO}_3$ ; filled triangles, loss on ignition (LOI). Lines associated with the excess  $^{210}\text{Pb}$  plots (Figs 6 and 7) represent linear regression plots.

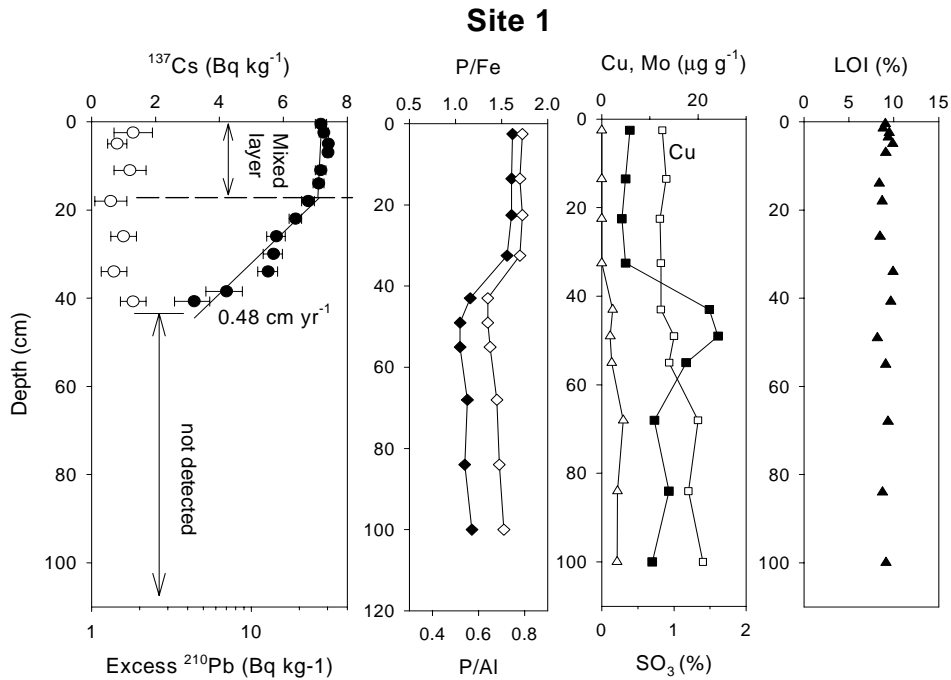


Fig. 10

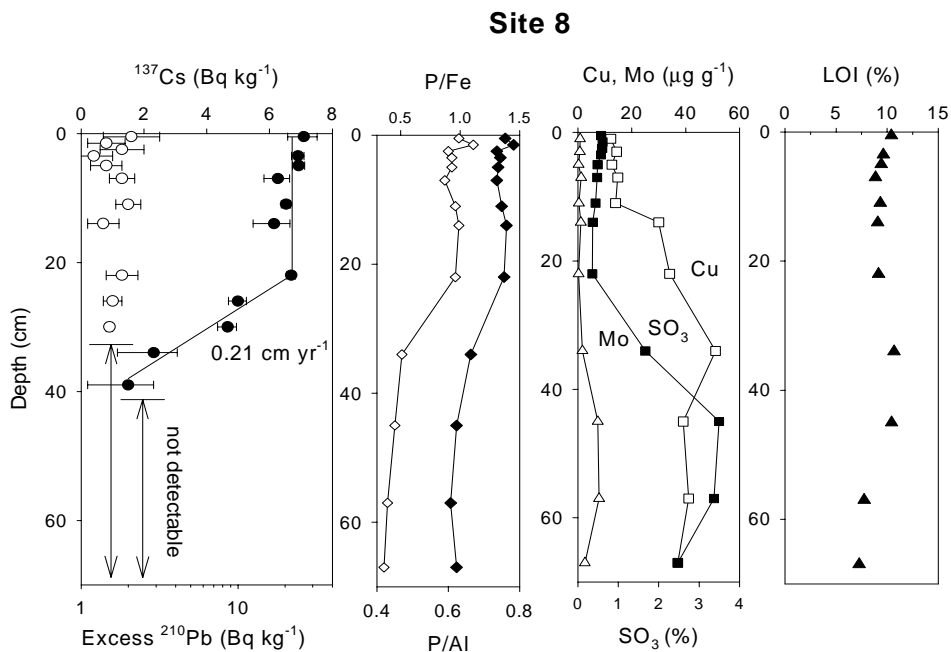


Fig. 11

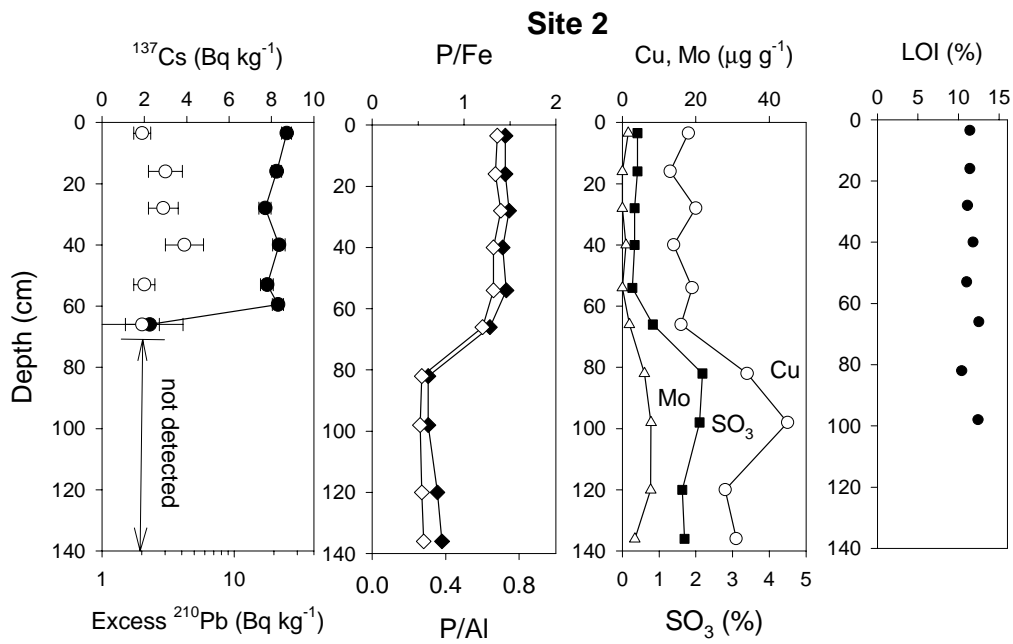


Fig. 12

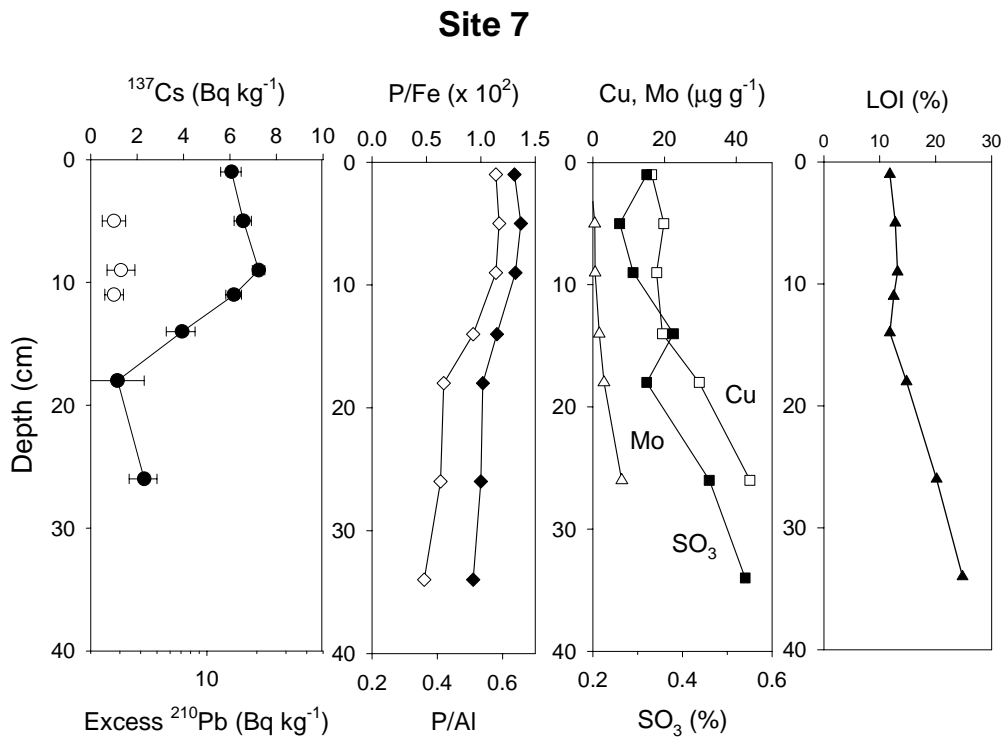


Fig. 13

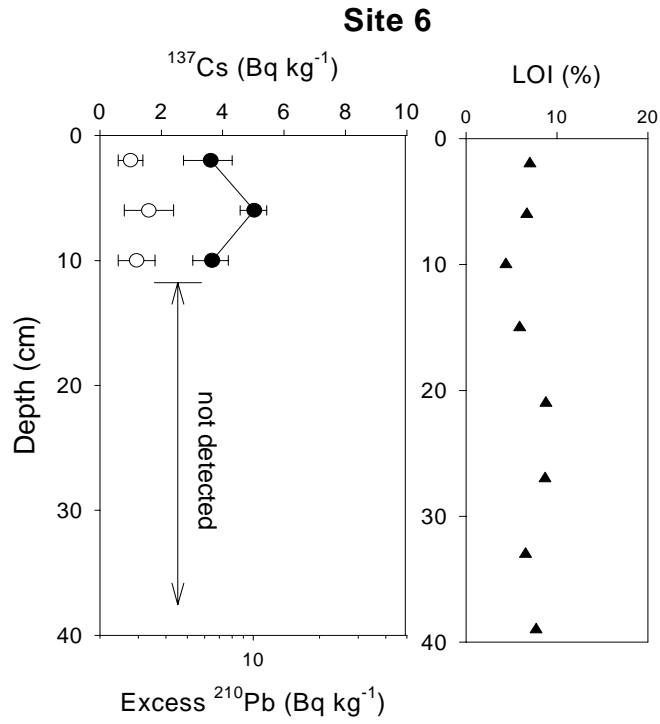


Fig. 14

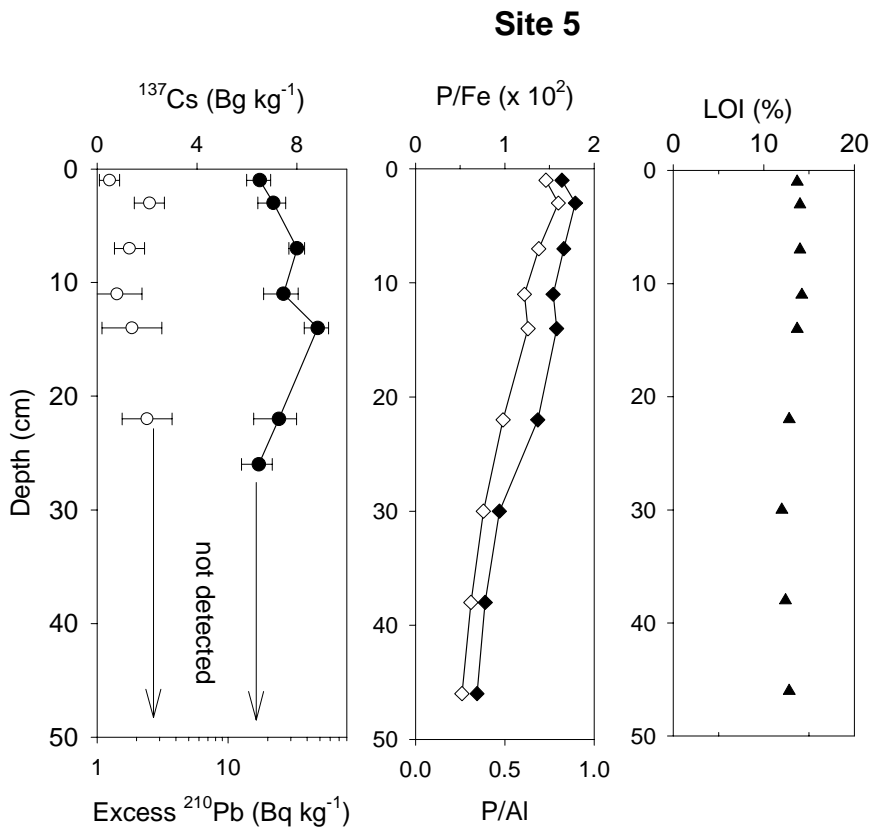
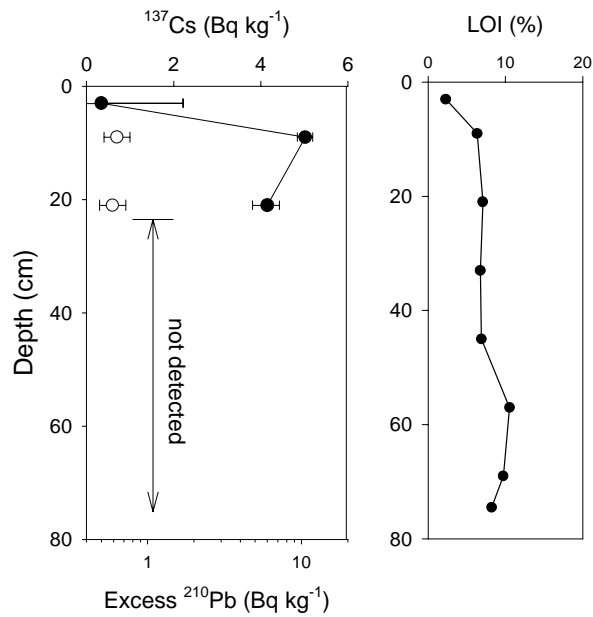


Fig. 15

### Site 4



**Fig. 16**

#### OSL

OSL dating was attempted on 5 cores. One or two layers were analysed from each core, each layer corresponding to a vertical depth interval of up to 10 cm. The entire sediment profile from site 1, and deep sediment from site 2 (>70 cm) was found unsuitable for OSL dating due to the lack of sand-sized quartz and feldspar grains.

Successful OSL dating results from four sites are given in Table 4. Dates are expressed as the minimum, maximum and mean ages of at least 40 small aliquot measurements. The age range in some depth sections is quite large, and may represent poor grain bleaching, or mixing of varying proportions of young and old sediment.

**Table 4. Results of OSL dating. Uncertainties in age determinations are due to analytical uncertainties.**

Site	Location	Depth (cm)	Min age (years)	Max age (years)	Mean age (years)
2	Corinella (north)	57-62	40 ±10	40 ±10	40 ±10
7	Upper North Arm (Lang Lang)	18-24	50 ±10	200 ±20	170 ±40
6	Upper North Arm (Yallock Ck)	10-18	30 ±10	4000 ±400	170 ±30
4	Upper North Arm (Charing Cross)	4-10	<10	420 ±60	45 ±6
		36-46	680 ±60	2340 ±270	1630 ±50

#### *Pinus pollen*

The relatively sensitive method of Ogden (1996) has been used to detect *Pinus* pollen in Western Port sediments. Given the sensitivity of the method, and the proximity of the Western Port catchment to a large population center (Melbourne), it is assumed that *Pinus* pollen would have been easily detectable in Western Port sediments by the late 1800's. A date of 1890 ( $\pm 10$  years) is assigned to the sediment horizon of first detection.

Two of the longest cores, from sites 1 and 2 (East Basin and Corinella north), were chosen for pollen determinations, as these were expected to provide the longest historical record of sedimentation, and because the alternative dating method, OSL, provided little or no chronological information for these cores. *Pinus* pollen concentration profiles are given in Table 5.

**Table 5. *Pinus* abundance in two cores from the East Arm.**

Location	Depth (cm)	<i>Pinus</i> pollen (grains g <sup>-1</sup> wet sediment)
Site 1 (East Basin)		
	7-13	30
	25-30	21
	35-40	12
	46-52	2
	58-64	1
	64-72	0
	72-80	0
	88-96	0
Site 2 (Corinella north)		
	7-13	24
	24-30	14
	43-49	13
	62-70	10
	70-78	4
	86-94	0
	102-110	0
	112-120	0

### 4.3 Core chronologies

In this section the chronology and sedimentation history of each core is evaluated and discussed. Discussion is ordered by location, from south to north, starting at site 1 (East Basin). Time horizons are shown in Fig. 9, and the chronologies are summarised in Table 6.

#### *Site 1 (East Basin)*

A combination of measurements from two adjacent cores are used to determine the sediment chronology at this site. The two cores include a short core (length 43 cm) and a long core (135 cm). The radionuclide profiles and the occurrence of a dense shell layer at 35-45 cm correlate well in both cores, and the two profiles are considered to be well matched. OSL dating of sediment from the long core was attempted but was unsuccessful due to the lack of sand-sized grains.

The 2-layer mixing model is applied to the excess  $^{210}\text{Pb}$  profile. Approximately constant excess  $^{210}\text{Pb}$  activity is seen in the upper 18 cm ( $\pm 2$  cm) of sediment (Fig. 10) and is assumed to be due to mixing. Below the mixed layer the log-linear plot of activity and depth is approximately linear. Applying a linear regression to the lower layer gives a mean accumulation rate over the last 60 years of  $0.48 \pm 0.05$  cm yr $^{-1}$ .

The  $^{137}\text{Cs}$  profile is consistent with the  $^{210}\text{Pb}$  accumulation rate. Cs-137 is seen to a depth of 42 cm, equivalent to a penetration depth of 24 cm below the mixed layer. The  $^{137}\text{Cs}$  estimate of sediment accumulation is therefore given by 24 cm/42 years, or  $0.57$  cm yr $^{-1}$ . Given the depth resolution of core sectioning (4 cm), and the uncertainty in thickness of the mixed layer ( $\pm 2$  cm), this accumulation rate is probably not significantly different to the  $^{210}\text{Pb}$ -derived rate.

Based on the excess  $^{210}\text{Pb}$  accumulation rate, sediment below 42 cm is older than about 50 years (pre-1950 A D). It should be recognised however, that sediment at 42 cm does not necessarily represent the characteristics of sediment deposited in 1950. Due to the homogenising effect of the mixing, sediment emerging from beneath the mixed layer exhibits a mixture of the characteristics of sediment deposited over a period of time equal to the time it takes sediment grains to move through the mixed layer. This time is equal to the depth of the mixed layer divided by the accumulation rate, and is 37 years at site 1 ( $18$  cm/ $0.48$  cm yr $^{-1}$ ). Thus sediment at 42 cm exhibits characteristics of sediment deposited over a 37 year period prior to 1950, ie. 1913-1950.

*Pinus* pollen at site 1 (Table 5) is abundant in the upper 42 cm of sediment at site 1. It becomes less abundant below 46 cm and is not detected below 64 cm. If sediment at 42 cm is dated at 1950, the horizon of first appearance of *Pinus*, dated at 1890, is 22 cm deeper. The mean accumulation rate between 1890 and 1944 is therefore  $0.37$  cm yr $^{-1}$  (22 cm/60 years). This rate is not much different to the apparent  $^{210}\text{Pb}$ - $^{137}\text{Cs}$  rate determined for the last 50 years, and indicates a reasonably constant accumulation rate over the last 100 years at this site.

#### *Site 8 (Corinella south)*

This core shows similar trends in excess  $^{210}\text{Pb}$  activity to site 1, and the 2-layer mixing model is applied. Constant excess  $^{210}\text{Pb}$  activity is seen to a depth of 22 cm indicating rapid mixing. The observation of brownish sediment to a depth of about 25 cm is also consistent with sediment oxidation induced by rapid mixing. Below 22 cm a linear regression of excess  $^{210}\text{Pb}$  activity and depth yields an accumulation rate of  $0.21 \pm 0.03 \text{ cm yr}^{-1}$ . As was the case at site 1, the  $^{137}\text{Cs}$  profile is consistent with the excess  $^{210}\text{Pb}$  estimate of accumulation. The maximum depth of  $^{137}\text{Cs}$  detection is 32 cm, or 10 cm below the mixed layer, yielding an average 42-year accumulation rate of  $0.24 \text{ cm yr}^{-1}$ .

Excess  $^{210}\text{Pb}$  is not detected below 36 cm, or 14 cm below the base of the mixed layer. Assuming an accumulation rate of  $0.21 \text{ cm yr}^{-1}$ , sediment below 36 cm is dated as being older than 67 years ( $14 \text{ cm}/0.21 \text{ cm yr}^{-1}$ ), or pre-1933.

#### *Site 2 (Corinella north)*

Excess  $^{210}\text{Pb}$  activity is approximately constant ( $\sim 20 \text{ Bq kg}^{-1}$ ) to a depth of 62 cm. The activity decreases rapidly below this depth and is not detected below 70 cm. The deepest detectable  $^{137}\text{Cs}$  activity occurs in the 57-62 cm depth interval.

The rapid disappearance of excess  $^{210}\text{Pb}$  below 62 cm does not allow for more than a very crude estimate of sediment accumulation. The lack of excess  $^{210}\text{Pb}$  below 70 cm indicates that this sediment is older than about three  $^{210}\text{Pb}$  half-lives (66 years, pre-1934). Applying the 2-layer mixing model with a 62 cm mixed layer gives an accumulation rate of  $<0.1 \text{ cm yr}^{-1}$ . However, such a deep layer of rapid mixing must be considered unlikely, given that the mixing depths at site 1 and site 8 are less than 25 cm.

An alternative explanation is that the layer of constant excess  $^{210}\text{Pb}$  activity represents a period of very rapid accumulation of sediment. This explanation is supported by OSL dating, and by the relatively high  $^{137}\text{Cs}$  inventory. The OSL technique gave a similar and very concise dose value (standard error 7%) for all aliquots of sand-sized sediment sampled from the 57-62 cm depth interval. This result indicates a very narrow age range. If the sediment in the upper 62 cm represented slow accumulation and post-depositional mixing a broad dose range reflecting a wide range of sediment ages would have been seen. Thus OSL dating of the 57-62 cm depth section ( $40 \pm 10$  years) indicates that the entire upper 62 cm has been deposited within the last 50 years, with an average accumulation rate of  $1.6 \pm 0.4 \text{ cm yr}^{-1}$ . The relatively high  $^{137}\text{Cs}$  inventory at this site shows that the amount of sediment that has accumulated since 1960 is much higher than other areas of the bay, in agreement with the OSL interpretation.

In summary, the  $^{210}\text{Pb}$ ,  $^{137}\text{Cs}$  and OSL chronologies are consistent with an age of 42 years or less for sediment above 62 cm, and indicate that substantial deposition of sediment has occurred at this site in the last 40 years.

*Pinus* pollen is plentiful to a depth of 62 cm. It is detected in smaller quantities between 62 and 78 cm and is not seen below 86 cm. This places the 1890 horizon

between 78 and 86 cm, and yields an accumulation rate of around  $0.3 \text{ cm yr}^{-1}$  for the period between 1890 and 1958.

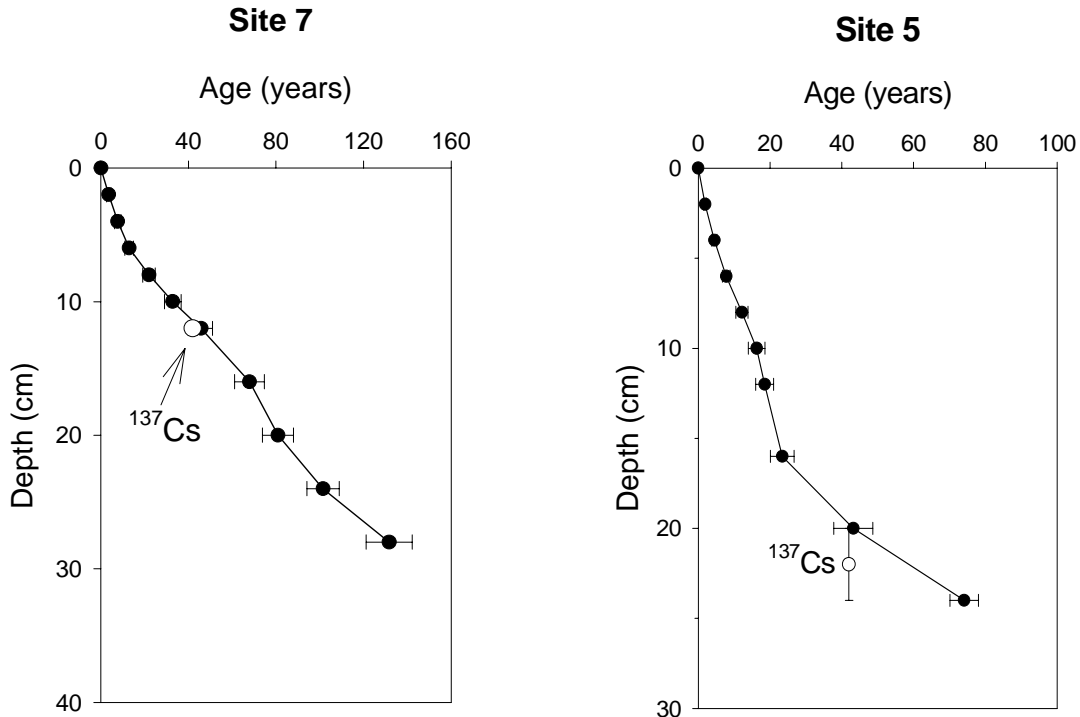
*Site 7 (near Lang Lang R. mouth)*

Sediment at site 7 overlies a dense layer of organic-rich peat-like material (described above), the proportion of which increases markedly below 20 cm. Excess  $^{210}\text{Pb}$  activity is not constant in the upper layers (Fig. 13), indicating that if vertical mixing is occurring at this site it is restricted to the upper few cm. Excess  $^{210}\text{Pb}$  activity decreases rapidly below 10 cm to a minimum at about 20 cm. It then increases slightly to low positive values between 20 and 32 cm.

A non-monotonic decrease of excess  $^{210}\text{Pb}$  with depth is often indicative of variable rates of sediment accumulation (Appleby and Oldfield, 1992). In these cases the CRS model is commonly used to determine a chronology. The model assumes a constant rate of  $^{210}\text{Pb}$  supply to the sediment, a doubtful assumption in a dynamic environment such as Western Port. Nevertheless, if approximately steady state conditions are assumed between supply of  $^{210}\text{Pb}$  by deposition of fine-grained particles, and loss by resuspension and transport to other areas of the bay, the model can serve as a useful starting point in constraining sediment ages. Application of this model yields the age versus depth plot shown in Fig. 17.

The CRS age profile agrees well with the first appearance  $^{137}\text{Cs}$  at 12 cm, giving an age of  $44 \pm 6$  years. The oldest CRS-dated sediment occurs at 28 cm, with an age of  $132 \pm 7$  years. The latter age should be treated with some caution, as  $^{210}\text{Pb}$  dating of sediment older than 100 years is less reliable than dating of younger sediment, especially where the assumptions of the dating model are questionable. Even so, some age constraints can be confidently applied. The agreement of  $^{210}\text{Pb}$  ages with the first appearance of  $^{137}\text{Cs}$  indicates that ages down to 12 cm are reasonable. OSL dating of the 18-24 cm depth interval yielded ages in the range 50-200 years. The youngest age is  $55 \pm 5$  years. This age compares reasonably with the nearest equivalent  $^{210}\text{Pb}$ -dated section (66 to 78 years in the 16-20 cm depth interval). If the minimum OSL age of 55 years is assumed to be associated with the uppermost portion of the 18-24 cm interval (say 18 cm), an accumulation rate of  $\sim 0.5 \text{ cm yr}^{-1}$  is indicated between 12 cm (dated at 1958 by  $^{137}\text{Cs}$ ) and 18 cm (dated at 1945 by OSL).

The maximum OSL age of 200 years in the 18-24 cm interval is not consistent with the  $^{210}\text{Pb}$  ages, as the presence of detectable excess  $^{210}\text{Pb}$  at 20-30 cm dates the mud fraction of sediment above 30 cm as less than 100 years old. Poorly bleached sand grains, or mixing of young sediment with sand grains from older deeper sediment are possible explanations for the disparity.



**Figs. 17 and 18.**  $^{210}\text{Pb}$  and  $^{137}\text{Cs}$  age versus depth plots at site 7 (left) and site 5 (right). Filled circles, CRS  $^{210}\text{Pb}$  ages; unfilled circles,  $^{137}\text{Cs}$  horizon. Error bars are determined by propagation of analytical uncertainties.

*Site 6 (near Yallock Ck. mouth)*

Excess  $^{210}\text{Pb}$  activity is low and limited to the upper 12 cm of sediment (Fig. 14). Neither excess  $^{210}\text{Pb}$  nor  $^{137}\text{Cs}$  are detected below 12 cm. In combination, the  $^{210}\text{Pb}$  and  $^{137}\text{Cs}$  activities indicate that sediment below 12 cm is older than 42 years.

OSL dating of the 10-20 cm interval yields an age range of 25-4000 years. If the youngest sediment is assumed to come from the uppermost portion of the interval (say 10 cm) the minimum OSL age of 25 years is consistent with the  $^{210}\text{Pb}$ - $^{137}\text{Cs}$  chronology. Again, OSL indicates that mixing of young and very old sand grains has occurred and the accumulation rate determined from  $^{210}\text{Pb}$  and  $^{137}\text{Cs}$  in the upper 12 cm ( $0.3 \text{ cm yr}^{-1}$ ) is therefore an upper limit.

*Site 5 (near Bunyip Drain mouth)*

The excess  $^{210}\text{Pb}$  profile at site 5 is similar to site 7; a sub-surface maximum (14 cm) decreasing to non-detectable activity below 28 cm (Fig. 15). Cs-137 activity is not detectable below 24 cm. Applying the CRS model gives an age versus depth plot

shown in Fig. 18. The oldest sediment able to be dated occurs at 24 cm, with an age of  $65 \pm 3$  years. The appearance of  $^{137}\text{Cs}$  in the 20-24 cm depth interval agrees within the bounds of the  $^{210}\text{Pb}$  chronology (35-68 years).

Based on this chronology, sediment at 24 cm is dated as 42-68 years and the accumulation rate for the upper 24 cm is  $0.35\text{-}55 \text{ cm yr}^{-1}$ .

#### *Site 4 (Charing Cross)*

Excess  $^{210}\text{Pb}$  and  $^{137}\text{Cs}$  are not detected below 18 cm (Fig. 16), dating this sediment as pre-1958. It is interesting to note the absence of excess  $^{210}\text{Pb}$  and  $^{137}\text{Cs}$  in the 0-6 cm interval. Given that this sediment must be younger than sediment below it, the lack of these two tracers indicates recent deposition of sediment not exposed to fallout tracers. This sediment must have come from a subsoil source; either remobilisation of buried marine sand, or subsoil erosion of the Westernport catchment.

The OSL age range for the 4-10 cm interval is  $<10$  to 420 years. Most of the age measurements were at the younger end of the age range, with a median age of  $45 \pm 6$  years. In combination, the OSL and  $^{210}\text{Pb}$  and  $^{137}\text{Cs}$  chronologies indicate a mixture of young and old sediment to a depth of 18 cm. The accumulation over the last 40 years rate is therefore less than  $0.4 \text{ cm yr}^{-1}$ .

The OSL age range for the 36-46 cm interval is 680-2340 years. The much greater age of this deeper layer shows that the effects of sediment influx over the last century is limited to sediment above 36 cm. The very large age range of quartz grains below 36 cm indicates relict marine sand deposited prior to European settlement.

#### **4.4 Major and trace elements**

Tables of selected major and trace elements for cores from sites 1, 5, 7 and 8 are given in the Appendix. Most elements show little change with depth. Exceptions are P, Cu and Mo, all of which show consistent trends at all sites. P shows a general decrease with depth. Plots of the mass ratio of P/Fe and P/Al are shown in Figs. 10, 11, 12, 13 and 14. P is normalised to both Fe and Al to correct for variation in particle size and clay- mineral content of the sediment. Al and Fe are usually good indicators of the clay mineral content of the bulk sediment, and due to their small particle size range ( $<2 \mu\text{m}$ ) clay minerals bind most of the available P in aquatic systems (Golterman, 1973), either by direct adsorption to particle surfaces, or bound to Fe-oxides coating the soil grains (Norrish and Rosser, 1983). The P/Fe and P/Al ratios both show similar trends; an increase in the upper layer of sediment at all sites where it they were measured, corresponding to an increase of 50-100% over deeper sediment.

**Table 6. Summary of core chronologies and historical accumulation rates.**

Site	Depth	Chronology	Accumulation rate
1	0-18 cm	Mixed layer; age range 0-37 years	Not known, but 0.48 cm yr <sup>-1</sup> assumed
	42 cm	Sediment below 42 cm is pre-1950.	0.48 cm yr <sup>-1</sup>
	64 cm	Sediment below 64 cm is pre-1890.	0.37 cm yr <sup>-1</sup>
8	0-22 cm	Mixed layer; age range 0-105 years	Not known, but 0.21 cm yr <sup>-1</sup> assumed
	22-36 cm	Sediment below 36 cm is pre-1950	0.21 cm yr <sup>-1</sup>
2	0-62 cm	Very rapid deposition	>1.6 cm yr <sup>-1</sup>
	62-86 cm	Sediment below 62 cm is pre-1958 Sediment below 86 cm is pre-1890	0.30 cm yr <sup>-1</sup>
7	0-12 cm	0-42 years; sediment below 12 cm pre-1958; old and young sand present	<0.30 cm yr <sup>-1</sup>
	12-18 cm	42-55 years	<0.50 cm yr <sup>-1</sup>
	18-30 cm	Transition into dense "peat" layer; 55 to <100 years;	>0.25 cm yr <sup>-1</sup>
6	0-12 cm	0-42 years; old and young sand present	<0.3 cm yr <sup>-1</sup>
5	0-24 cm	0-42 years	0.35-0.55 cm yr <sup>-1</sup>
4	0-18 cm	0 to 42 years; old and young sand present	<0.4 cm yr <sup>-1</sup>
	36 cm	Sediment below 36 cm >680 years.	n.d.

Although these higher levels of P are associated with sediment deposited in the bay over the last 40 years (based on the chronologies determined above) it is noted that the elevated concentrations of P are not high compared to natural levels of P in soils (Norrish and Rosser, 1983). Moreover, it is not known whether the elevated P is derived directly from the Westerport catchment, or whether it has accumulated in the upper layer of sediment as a result of *in-situ* biological activity and/or desorption of organic matter (dead plankton). Enrichment of organic matter in the upper sediment layer would lead to elevated levels of P. The required increase in organic matter, which is approximately 1% P dry weight, would not need to be more than a few % of the total sediment mass to account for the observed elevation in P, and would not be easy to detect using LOI measurements. The origin of this elevated P is the subject of further investigation.

Cu, Mo and S are plotted in Figs 10,11,12 and 13. Both show a concentration increase at some point in the sediment profile, although the trend at site 1 is weak. At site 2, Cu concentrations reach a maximum at 100 cm, and decrease at greater depths.

Molybdenum shows similar trends to Cu. The cause of these variations is uncertain, although the correlation of Cu and Mo with S indicates diagenesis is likely, ie. diffusion, dissolution and precipitation of various chemical phases due to changing redox conditions in the sediment profile. Cu and Mo are known for their ability to be incorporated into sulphides in anoxic sediments (Calvert, 1976). The elevated concentrations do not appear to be of anthropogenic origin as they extend well below

the *Pinus* 1890 horizon, putting them in a historical period not readily associated with the onset of industrial activities in Westernport.

## 5. Discussion

Fig. 19 is a schematic summarising sediment accumulation determined from the above chronologies. The accumulation rates indicated are upper limits.

### 5.1 East Arm Sites

The accumulation of mud at East Arm sites is up to an order of magnitude higher than at Upper North Arm sites, based on excess  $^{210}\text{Pb}$  inventories, apparent  $^{210}\text{Pb}$ - $^{137}\text{Cs}$  accumulation rates, and the fact that sediment at the East Arm sites is almost entirely composed of fine-grained silt and clay (<98% mud). The accumulation rate of sediment at site 1 (East Basin,  $0.48\text{ cm yr}^{-1}$ ) is equivalent to  $2.5\text{ kg m}^{-2}\text{ yr}^{-1}$ , based on the porosity (0.75) and sediment dry density ( $2.1\text{ g cm}^{-3}$ ) at this site. An approximate depositional load for the East Basin can be determined if it assumed that this core represents sediment accumulation in the mud-rich areas of the Basin. Applying the site 1 accumulation rate to the mud-rich area within the East Basin ( $33\text{ km}^2$ , the area defined by the 50-95% mud contour, containing an average 60% mud) gives a mud depositional load of  $49\text{ kt yr}^{-1}$  (60% of  $33\text{ km}^2 \times 2.6\text{ kg m}^{-2}\text{ yr}^{-1}$ ). An approximate contour of the East Basin is shown by the area drawn in the  $<63\text{ }\mu\text{m}$  distribution in Fig. 4, and is defined by water depth  $>3\text{ m}$ . If the mud content of the entire basin is considered (area  $64\text{ km}^2$ , average 50% mud) a load of  $80\text{ kt yr}^{-1}$  is calculated.

Applying the  $^{210}\text{Pb}$  estimate of sediment accumulation at site 8 (Corinella south,  $0.21\text{ cm yr}^{-1}$ , or  $1.1\text{ kg m}^{-2}\text{ yr}^{-1}$ ) to the area of mud-rich sediment within the Corinella segment (area  $30\text{ km}^2$ ) gives a total fine-grained depositional load of  $20\text{ kt yr}^{-1}$ . The sum of the East Basin and Corinella depositional load estimates lies between 70 and  $100\text{ kt yr}^{-1}$ . However, it is acknowledged that this depositional load estimate is based on extrapolations from just two cores which may not represent a wider deposition zone, and that a significant degree of uncertainty is associated with the estimate.

An interesting feature of all East Arm cores is the occurrence of discrete beds of coarse shell fragments. The beds, which cover a depth interval of about 20 cm, are dated as post 1890 at their base (sites 1 and 2). The beds span the 1960 time horizon, although the effect of mixing in the upper the layer would suggest that the input of shells into surficial sediment may have diminished well before this. It is not known if the beds represent different bottom sediment regime ecology in the past, or are a product of bioturbation. The concentration of shell fragments increases immediately below the mixed layer, but if bioturbation is responsible for the transport of shell from the mixed layer into deeper sediment, and the supply of shell fragments has remained plentiful, a continuous distribution of shells of unchanging concentration would be expected immediately below the mixed layer. The occurrence of a discrete layer suggests a changing supply of shell fragments to the East Arm over the last 100 years.

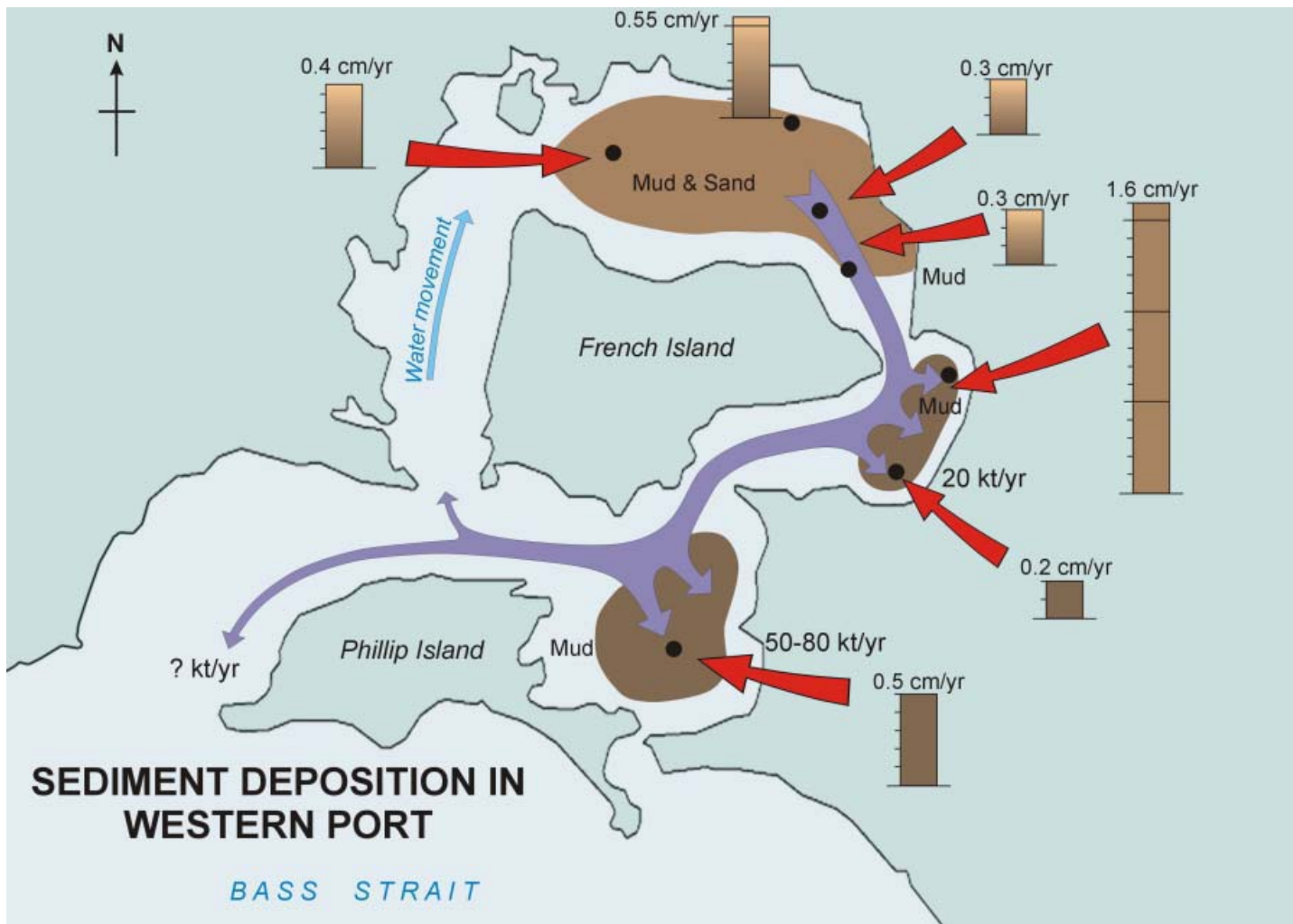


Fig. 18. Schematic of sediment accumulation in Western Port. Sediment accumulation rates are upper limits

## 5.2 Upper North Arm

Sediment profiles at sites 4, 5, 6 and 7 show that the sediment that has accumulated over the last 40-60 years in the Upper North Arm is confined to a layer 12 to 24 cm thick. The maximum accumulation rate is 0.3-0.4 cm yr<sup>-1</sup> at most sites, but it may be as high as 0.55 cm yr<sup>-1</sup> at the Bunyip Drain outlet. Table 4 shows that a mix of 'young' (<50 years) and 'old' (>200 years) sand occurs in all OSL-dated sediment from the Upper North Arm. These older ages are consistent with a relict marine source, and suggest that deposited sand is a mixture of old reworked marine sand and recent input of well bleached (young) sand from the catchment. The spatial origin of the relic sand is not known, but the very low activities of excess <sup>210</sup>Pb and <sup>137</sup>Cs in the surface 4 cm of the core from site 4 (Charring Cross) indicates a recent "dump" of sand, the immediate origin of which is almost certainly subsurface (Wallbrink et al., 1999). Subsurface sand might include eroded subsoil in the Westerport catchment, or lateral transport of old deep sediment exposed by erosion within the bay.

The range of OSL ages of sand grains in the Upper North Arm suggests a process whereby old and young sand grains are being mixed. The non-constant excess <sup>210</sup>Pb activity seen in the upper layers of most of the Upper North Arm cores indicates that vertical mixing within the sediment profile, if occurring, is limited to just the upper few cm. However, given the dynamic nature of water movement in the shallow regions of the bay, lateral mixing of old and young sand prior to deposition resulting from resuspension and transport, is also a distinct possibility. This lateral transport, or "smearing" of old and young sand around the Upper North Arm may be a continual process, or it may be episodic, occurring as a result of significant events in the bay (large tides, storms etc). Whatever the frequency of the process, mixing of sediment, whether lateral or vertical, would have the same effect on the apparent accumulation rate; ie. it would cause an over-estimate of net mass deposition by allowing downward movement of <sup>137</sup>Cs and excess <sup>210</sup>Pb. The implication of this diagnosis is that the apparent sediment accumulation rates in the Upper North Arm should be considered upper limits with regard to catchment input.

A feature of all Upper North Arm cores is the change in sediment composition with depth, indicating a change in the characteristics of sediment being delivered to Western Port and/or a changing depositional environment. All Upper North Arm cores show evidence of a trend towards a higher sand content over the last 40-60 years, and possibly longer (Fig. 9). By contrast, the silt/clay content at sites 4, 5 and 6 has decreased by a factor of about three over the same period. OSL dating suggests that a finite fraction of the upper layer of sand deposits in the Upper North Arm has been recently delivered from the Westerport catchment. An increase in the rate of delivery of catchment-derived sand over the last few decades may explain the higher sand content of the upper layers of sediment in the Upper North Arm. On the other hand, there is strong evidence presented in this study for widespread resuspension of mud in the Upper North Arm, and the relocation of some of it to the East Arm. Recent increases in the rate of removal of mud from the Upper North Arm, perhaps as a result of loss of seagrass meadows, would also explain the observed trend towards coarser sediment composition. It is likely that both these processes have influenced the particle size characteristics of sediment accumulated in the Upper North Arm over the last 40 years, but without more extensive core and suspended particle analysis it is not

possible to determine which process (sand influx or particle resuspension) is primarily responsible.

## 6. Summary and Conclusions

A combination of particle tracers, fallout chronometers, and OSL and *Pinus* pollen dating techniques have been used to study sediment transport and accumulation in Western Port bay. The following conclusions are drawn.

- Suspended particle residence times are short (of the order of 1-2 tidal cycles) indicating a dynamic process of resuspension and removal of fine-grained sediment (mud). Sediment inventories of the fallout tracers  $^{210}\text{Pb}$  and  $^{137}\text{Cs}$  indicate a relocation of fine-grained (silt/clay) sediment from the Upper North Arm in a clockwise southerly direction.
- Mud is focused in the East Arm. Comparison of the spatial distribution of sediment grain size undertaken by this study with a similar map published in the 1970's indicates a net loss of mud from the Upper North Arm over the last 25 years.
- The accumulation rate of mud is greatest in the East Basin. Sediment in this zone is apparently vertically mixed to a depth of 20 cm. When averaged over a time scale of a few decades, the sediment accumulation rate in this segment has not deviated much outside a range of 0.4-0.5 cm yr<sup>-1</sup> over the past 100 years. When applied to mud-rich zones in the east Arm these rates yields a depositional load of mud in the East Arm of 70 to 100 kt yr<sup>-1</sup>.
- Sediment accumulation in the Corinella segment appears more variable, with two cores yielding accumulation rates of 0.2 and 1.6 cm yr<sup>-1</sup> over the past 40 years.
- In the Upper North Arm influx of sediment during the last 40 to 60 years is confined to a sediment layer 12 to 24 cm thick. This yields an accumulation rate, averaged over the last few decades, of 0.3-0.5 cm yr<sup>-1</sup> for this segment. Due to the possibility of sediment reworking these estimates are upper limits with regard to catchment input.
- Upper North Arm cores show a transition to higher sand and lower silt/clay composition over the last 40-60 years. This could be due an increase in the rate of sand supply to the Upper North Arm from the Westernport catchment over the last few decades, or an increase in the rate of removal (resuspension and transport) of mud, or a combination of both processes.
- Generally P concentrations are enhanced by 50-100% in recent (<60 year old) sediment. This could be due to an increase in the P load delivered to the bay, or the presence of higher concentrations of organic matter in the upper sediments. This is being investigated further. Higher concentrations of Cu and Mo are seen in older sediments, but this appears to due be to diagenesis (sulphide formation) caused by anoxic conditions within the sediment profile.

## References

- Aitken M.J. (1998). An Introduction to Optical Dating. Oxford Univ. Press, Oxford.
- Appleby, P.G. and Oldfield F. (1992). Application of lead-210 to sedimentation studies. In: *Uranium-series Disequilibrium: Applications to Earth, Marine and Environmental Sciences*, M. Ivanovich and R.S. Harmon eds., 731-778, Clarendon press, Oxford.
- Berger, W.H. and Heath, G.R (1968). Vertical Mixing in Pelagic Sediments. *Journal of Marine Research*, **26**, 134-143.
- Calvert, S.E. (1976). Mineralogy and geochemistry of near-shore sediments, In J.P. Riley and R. Chester (eds.), *Chemical Oceanography*, Vol. 6, 2<sup>nd</sup> Edn. Academic press, London, pp 187-280.
- Fielding, J.M. (1957). *Pinus* in Australia. *Australian Forestry* **21**, 15-16.
- Golterman, H.L. (1973). Vertical movement of phosphate in freshwater. In: *Environmental Phosphorus Handbook*, E.J. Griffith, A.L Beeton, J.M. Spencer and D.T. Mitchell eds., 509-538, Wiley, New York.
- Hancock G.J. and Hunter J.R. (1999). Use of excess <sup>210</sup>Pb and <sup>228</sup>Th to estimate rates of sediment accumulation and bioturbation in Port Phillip Bay, Australia. *Marine and Freshwater Research*, **50**, 533-45.
- Hancock, G.J., Webster, I.T., Ford, P.F. and Moore W.S. (2000). Using Ra isotopes to examine transport processes controlling benthic fluxes into a shallow estuarine lagoon. *Geochimica et Cosmochimica Acta*, **64**, 3685-3699.
- Harris, J.E. and Robinson, J.B. (1979). Circulation in Western Port, Victoria, as deduced from salinity and reactive-silica distributions. *Marine Geology*, **30**, 101-116.
- Harris, J.E., Hinwood, J.B., Marsden, M.A.H. and Sternberg, R.W. (1979). Water movements, sediment transport and deposition, Western Port, Victoria. *Marine Geology*, **30**, 131-161.
- Hinwood, J.B. (1979). Hydrodynamic and transport models of Western Port, Victoria. *Marine Geology*, **30**, 117-130.
- Huntley, D.J., Godfrey-Smith D.I. and Thewalt M.L.W. (1985). Optical dating of sediments. *Nature* **313**, 105-107.
- Lowe, M. (1999). Sediment sources in Western Port catchment. Honours thesis. University unknown, 47 pp.
- May, D. and Stephens, A. (1996). The Western Port Marine Environment. Publication 493, Environment Protection Authority, Victoria.
- Martin, P. and Hancock, G. J. (1992). Routine analysis of naturally occurring radionuclides in environmental samples by alpha-particle spectrometry, Research Report 7, Supervising Scientist for the Alligator Rivers Region, AGPS, Canberra, Australia.
- Marsden, M.A.H. (1979). Circulation patterns from seabed-drifter studies, Western Port and inner Bass Strait, Australia. *Marine Geology*, **30**, 85-99.

- Marsden, M.A.H. and Mallet, C.W. (1975). Quaternary evolution, morphology, and sediment distribution, Westernport Bay, Victoria. *Proceedings of the Royal Society of Victoria*, **87**, 107-138.
- Marsden, M.A.H., Mallet, C.W. and Donaldson, A.K. (1979) Geological and Physical setting, sediments, and environments, Western Port, Victoria. *Marine Geology*, **30**, 11-46.
- Murray A.S. and Mejdahl V. (1998). Comparison of regenerative-dose single-aliquot and multiple-aliquot (SARA) protocols using heated quartz from archaeological sites. *Quaternary Science Reviews* (in press).
- Murray A.S. and Roberts R.G. (1998). Measurement of the equivalent dose in quartz using a regenerative-dose single-aliquot protocol. *Radiation Measurements*, **29**, 503-515.
- Murray A.S., Marten, R., Johnson, A. and Martin, P. (1987). Analysis for naturally occurring radionuclides at environmental concentrations by gamma spectrometry. *Journal of Radioanalytical and Nuclear Chemistry Articles*, **115**, 263-288.
- Norrish, K., and Hutton J.T. (1969). An accurate X-ray spectrographic method for the analysis of a wide range of geological samples. *Geochimica et Cosmochimica Acta* **33**, 431-453.
- Norrish, K., and Chappell B.W. (1977). X-ray fluorescence spectrometry. In 'Physical methods in determinative mineralogy', second edition, ed. J. Zussman (Academic Press: London), 201-272.
- Norrish, K., and Rosser, H. (1983). Mineral Phosphate, In: *Soils: An Australian Viewpoint*. Division of Soils, CSIRO, pp 335-361, CSIRO Melbourne.
- Ogden, R.W. (1996). The impact of farming and river regulation on billabongs of the southeast Murray Basin, Australia. PhD thesis, Australian National University, Canberra. 396 pp.
- Ogden, R.W. (2000). Modern and historical variation in aquatic macrophyte cover of billabongs associated with catchment development. *Regulated Rivers: Research and Management*, **16**, 497-512.
- Olive, L. J., Olley, J. M., Murray, A. S. and Wallbrink, P. J. (1995). Variations in sediment transport at a variety of temporal scales in the Murrumbidgee River, New South Wales, Australia. In: *Effect of Scale on Interpretation and Management of Sediment and Water Quality* (Proceedings of Boulder Symposium, July, 1995). IAHS Publication no. 226, 275-284.
- Olley, J. M., Murray, A. S., Wallbrink, P. J., Stanton, R. K. and Caitcheon, G. G. (1990). The use of Fallout nuclides as chronometers. Quaternary dating workshop, A.N.U., Aug. 1990, pp 51-55.
- Roberts R., Bird M., Olley J., Galbraith R., Lawson E., Laslett G., Yoshida H., Jones R., Fullagar R., Jacobsen G. and Hua Q. (1998). Optical and radiocarbon dating at Jinmium rock shelter in northern Australia. *Nature* **393**, 358-362.
- Sargeant, I. (1977). A review of the extent and environmental effects of erosion in the Westernport catchment. Environmental Studies Series Publication No.174. Ministry for Conservation, Victoria.
- Shapiro, M.A. (1975). Westernport Bay environmental study 173-1974. Ministry for Conservation, Victoria, Australia.

- Turekian, K. K., Nozaki, Y., and Benninger, L. K. (1977). Geochemistry of atmospheric radon and radon products. *Annual Review Earth Planet Science* **5**, 227-255.
- Wallbrink, P.J., Murray, A.S. and Olley, J.M. (1999). Relating suspended sediment to its original soil depth using fallout radionuclides. *Soil Science of America Journal*, **63**, 369-378.
- Wilk, R.R. Keene, J.B. and Marden, M.A.H. (1979). Sediment characteristics in the embayment head of Western Port – The impact of swamp drainage and erosion on sedimentation and seagrass distribution. Environmental Studies Series Publication No. 24, Ministry for Conservation, Victoria.

## Appendix

Table A1. Radionuclide ( $\text{Bq kg}^{-1}$ ), LOI and porosity data. Radionuclide uncertainties ( $\pm 1$  SD) are given in small font.

### Site 1. East Basin

Depth (cm)	porosity	LOI (%)	$^{137}\text{Cs}$	$^{210}\text{Pb}$	$^{226}\text{Ra}$	$^{210}\text{Pb}$ excess
<b>Short core</b>						
0-1	0.83	9.1	0.2 0.6	48.5 1.5	21.1 1.6	27.4 2.2
1-2	0.80	8.8	0.2 0.6		24.0 1.6	
2-3	0.80	9.5	1.3 0.6	50.6 1.6	22.1 1.0	28.5 1.9
3-4	0.79	9.4	0.4 0.6		23.0 1.2	
4-6	0.78	9.9	0.8 0.3	53.2 1.3	22.8 0.8	30.4 1.5
6-8	0.76	9.1	0.5 0.5	53.3 1.2	23.0 1.0	30.3 1.6
10-12	0.75	10.6	1.2 0.5	50.0 1.9	22.7 0.8	27.3 2.1
12-16	0.74	8.4	0.6 0.6	49.3 1.9	22.8 1.0	26.5 2.1
16-20	0.72	8.7	0.6 0.5	47.5 1.9	24.7 0.8	22.8 2.1
20-24	0.70		0.5 0.5	43.7 1.5	24.7 0.8	19.0 1.7
24-28	0.67	8.5	1.0 0.4	40.4 1.8	26.0 0.6	14.4 1.9
28-32	0.67		1.0 0.2	39.5 1.4	25.7 0.4	13.8 1.5
32-36	0.66	9.9	0.7 0.4	38.3 1.7	25.5 0.7	12.8 1.8
36-39	0.62			30.7 1.3	23.7 1.4	7.0 1.9
39-42.5	0.61	9.7	1.3 0.4	28.1 0.8	23.7 0.8	4.4 1.1
<b>Long core</b>						
0-5	0.78	9.8	2.4 0.5	55.9 3.6	22.9 0.6	33.0 3.4
11-16	0.74	8.7	2.8 0.6	55.4 4.3	25.9 0.7	29.5 4.1
20-25	0.72	8.0	1.4 0.4	50.4 4.1	27.0 0.6	23.4 3.9
30-35	0.70	9.0	1.8 0.6	35.5 1.0	26.9 0.7	8.6 1.2
35-40				26.9 1.1	25.6 0.7	1.3 1.3
40-46		7.6	0.7 0.5	23.2 0.8	25.4 0.7	-2.2 1.1
46-52	0.72	8.2	0.5 0.3			
52-58	0.75	9.1	0.4 0.5	28.1 0.9	30.1 0.7	-2.0 1.2
64-72		9.4	0.5 0.4			
80-88	0.76	8.7	0.5 0.5	31.7 1.3	32.6 0.5	-0.9 1.4
96-104	0.75	9.1	0.3 0.4			
112-120	0.75	9.6	0.7 0.4			

Table A2  
Site 2. Corinella South

Depth (cm)	Porosity	LOI (%)	<sup>137</sup> Cs	<sup>210</sup> Pb	<sup>226</sup> Ra	<sup>210</sup> Pb
0-1	0.86	10.4	1.6 0.9	48.8 5.3	22.4 1.9	26.4 5.6
3-4	0.81	9.6	0.4 0.6	48.7 1.8	24.5 1.2	24.2 2.2
4-6	0.78	9.4	0.8 0.5	48.1 2.0	23.6 1.0	24.5 2.2
6-8	0.76	8.9	1.3 0.4	43.3 3.2	25.3 0.8	18.0 3.3
10-12	0.77	9.3	1.5 0.4	48.1 1.0	27.8 1.0	20.3 1.4
12-16	0.78	9.1	0.7 0.5	40.0 4.4	23.0 0.8	17.0 4.5
20-24	0.77	9.2	1.3 0.5	46.0 1.2	24.1 0.8	21.9 1.4
24-28	0.77		1.0 0.3	33.5 1.2	23.5 0.5	10.0 1.3
28-32	0.76		0.9 0.1	30.2 1.2	21.6 0.3	8.6 1.2
32-36	0.73	10.7	0.6 0.5	23.5 0.9	20.6 0.8	2.9 1.2
36-42	0.75		0.5 0.2	21.1 0.9	19.5 0.5	2.0 0.9
42-48	0.75	10.4	0.4 0.4	18.3 0.7	17.3 0.6	1.0 0.9
54-60	0.76	7.8	0.3 0.4	18.3 0.8	22.5 0.6	-4.2 1.0
64.5-69	0.77	7.3	-0.3 0.6	18.7 0.9	23.0 1.0	-4.3 1.3

Table A3  
Site 2. Corinella North

Depth (cm)	Porosity	LOI (%)	<sup>137</sup> Cs	<sup>210</sup> Pb	<sup>226</sup> Ra	<sup>210</sup> Pb excess
0-7	0.70	11.4	1.9 0.4	54.3 2.1	29.3 0.7	25.0 2.2
13-19	0.78	11.4	3.0 0.8	48.5 1.4	27.5 1.1	21.0 1.8
25-31	0.72	11.1	2.9 0.7	45.0 1.4	27.8 1.2	17.2 1.8
37-43	0.69	11.8	3.9 0.9	51.4 2.1	29.5 1.2	21.9 2.4
49-57	0.68	11.0	2.0 0.5	49.4 1.8	31.6 0.8	17.8 2.0
57-62			1.9 0.8	49.8 1.8	28.3 1.0	21.5 2.1
62-70	0.66	12.5	0.5 0.4	29.1 1.4	26.8 1.1	2.3 1.8
70-78			0.0 0.4	21.1 1.2	25.4 0.6	-4.3 1.3
78-86	0.84	10.4	-0.1 0.4	21.7 0.9	25.4 0.6	-3.7 1.1
94-102	0.85	12.4	0.3 0.3		26.1 0.6	
116-124	0.84		0.3 0.2		38.7 0.6	
132-140	0.85				38.8 0.6	
148-156	0.73				41.7 0.4	

Table A4  
Site 7 (near Lang Lang River).

Depth (cm)	Porosity	LOI (%)	<sup>137</sup> Cs		<sup>210</sup> Pb		<sup>226</sup> Ra		<sup>210</sup> Pb excess	
0-2	0.79	11.8	0.3	0.5	43.3	1.8	29.2	1.1	14.1	2.0
4-6	0.81	12.8	1.0	0.5	47.9	1.8	31.3	1.2	16.6	2.0
8-10	0.81	13.2	1.3	0.6	47.0	1.5	26.4	1.3	20.6	1.8
10-12	0.78	12.5	1.0	0.4	40.0	1.3	25.4	1.0	14.6	1.6
12-16	0.79	11.8	0.3	0.5	32.2	1.1	25.1	0.8	7.1	1.4
16-20	0.79	14.8	0.5	0.7	24.3	0.9	21.4	1.1	2.9	1.3
24-28	0.83	20.2	0.3	0.4	20.2	0.5	16.0	0.7	4.2	0.8
32-36	0.86	24.8	-2.1	4.4	14.2	0.6	9.6	0.9	3.0	0.9

Table A5  
Site 6 (near Yallock Ck.).

Depth (cm)	porosity	LOI (%)	<sup>137</sup> Cs		<sup>210</sup> Pb		<sup>226</sup> Ra		<sup>210</sup> Pb excess	
0-4	0.61	7.01	1.0	0.4	33.6	1.3	27.2	0.9	6.4	1.6
4-8	0.58	6.68	1.6	0.8	31.4	1.0	21.3	1.0	10.1	1.4
8-12	0.49	4.38	1.2	0.6	23.7	0.8	17.2	0.9	6.5	1.2
12-18	0.48	5.90	0.7	0.7	22.1	1.0	23.0	0.9	-0.9	1.3
18-24	0.49	8.78	0.0	0.3	35.5	1.8	37.2	1.4	1.7	2.5
24-30	0.54	8.69	0.1	0.3	42.9	1.2	45.9	0.5	3.0	1.0
30-36	0.49	6.54	0.0	0.2	46.2	1.5	49.1	1.5	-2.9	2.4
36-42	0.48	7.70	-0.1	0.3	49.0	2.8	52.9	1.6	-3.9	3.2

Table A6  
Site 5 (near Bunyip Drain).

Depth (cm)	Porosity	LOI (%)	<sup>137</sup> Cs		<sup>210</sup> Pb		<sup>226</sup> Ra		<sup>210</sup> Pb excess	
0-2	0.47	13.7	0.5	0.4	100	2	82.2	0.6	20.2	3.6
2-4	0.41	14.0	2.1	0.6	119	5	97.3	1.4	25.7	5.3
6-8	0.40	14.0	1.3	0.6	107	5	73.4	1.3	39.0	4.6
10-12	0.37	14.2	0.8	1.0	100	9	73.2	1.6	30.8	7.8
12-16	0.36	13.7	1.4	1.2	126	11	77.7	2.1	55.7	10.2
20-24	0.32	12.0	2.0	1.0	96	10	71.2	1.9	27.7	8.8
24-28			0.5	1.0	48.4	3.9	33.2	1.7	17.1	4.5
28-32	0.39	12.8	1.0	1.1	38.4	6.7	33.3	1.7	5.8	6.0
36-40	0.46	12.7	0.3	0.5	21.9	5.1	27.7	0.9	-6.6	4.7
44-48	0.51	12.4	0.4	0.8	29.5	4.9	28.8	1.2	0.8	4.3

Table A7  
Site 4. Charing Cross.

Depth (cm)	porosity	LOI (%)	<sup>137</sup> Cs	<sup>210</sup> Pb	<sup>226</sup> Ra	<sup>210</sup> Pb excess
0 – 6	0.53	2.30	0.2 0.2	12.0 0.6	12.7 0.4	-0.7 0.7
6 – 12	0.67	6.35	0.7 0.3	27.4 1.1	16.8 0.5	10.6 1.2
18 – 24	0.66	7.08	0.6 0.3	23.4 1.1	17.4 0.5	6.0 1.2
30 – 36	0.60	6.76	0.8 0.4	14.9 2.9	13.1 0.5	0.9 2.9
42 – 48	0.74	6.90	-0.3 0.4	24.7 3.4	22.4 0.6	0.6 3.5
54 – 60	0.77	10.5	0.2 0.5	23.7 3.7	23.9 0.7	-3.0 3.8
66 – 72	0.76	9.74	1.5 0.6	26.7 4.3	22.9 0.8	1.3 4.4
72 – 77	0.71	8.22	0.9 0.4	21.4 4.3	19.2 0.7	0.5 4.4

Table A8. Major element (%) and trace element ( $\mu\text{g g}^{-1}$ ) concentrations. Sites 1 and 2.

	SiO <sub>2</sub>	Al <sub>2</sub> O <sub>3</sub>	P <sub>2</sub> O <sub>5</sub>	TiO <sub>2</sub>	Fe <sub>2</sub> O <sub>3</sub>	SO <sub>3</sub>	Ni	Cu	Zn	Ga	Ge	As	Rb	Sr	Y	Zr	Nb	Mo	Cd	Sn	Ba	La	Ce	Nd	Yb	Hg	Pb	
<b>Site 1</b>	%	%	%	%	%	%																						
0-5	64.5	13.1	0.13	1.3	4.8	0.39	16	12	91	14	< 0.4	23	66	153	35	442	24	< 0.5	1.3	5	239	29	56	33	14	< 1.5	21	
11-16	66.3	12.2	0.12	1.3	4.5	0.33	8	12	76	10	5	23	64	163	36	455	24	< 0.5	1.6	4	253	33	62	41	29	< 1.5	21	
20-25	67.0	11.8	0.11	1.3	4.4	0.28	5	9	59	10	2	24	61	178	37	480	23	< 0.5	< 0.3	4	258	35	58	42	36	< 1.5	21	
30-35	66.3	11.7	0.11	1.3	4.4	0.33	5	9	57	9	2	23	61	184	37	526	23	< 0.5	1.2	3	241	33	65	31	27	< 1.5	21	
40-46	64.9	11.7	0.09	1.3	4.9	1.49	7	15	57	11	3	25	59	214	34	456	24	2.3	1.0	4	241	36	54	34	30	< 1.5	18	
46-52	61.5	14.7	0.11	1.8	6.7	1.61	11	15	47	16	2	29	64	150	34	353	30	1.8	0.6	3	235	32	61	47	67	< 1.5	20	
52-58	59.5	16.5	0.13	2.0	7.7	1.17	37	14	59	16	3	35	65	118	33	308	33	2.1	0.4	4	239	32	67	45	26	< 1.5	17	
64-72	59.7	16.6	0.14	2.0	7.6	0.73	29	20	57	15	< 0.4	24	67	120	35	307	35	4.5	0.3	3	252	32	64	51	31	< 1.5	19	
80-88	60.0	16.5	0.14	2.1	7.8	0.93	32	18	54	20	4	37	69	115	34	317	35	3.3	0.7	4	264	32	62	41	20	< 1.5	16	
96-104	59.3	16.8	0.15	2.1	7.7	0.70	28	21	62	19	2	29	67	114	34	300	34	3.2	0.4	5	250	21	56	< 3.0	14	< 1.5	18	
112-120	59.2	17.0	0.15	2.1	7.8	0.69	31	17	61	17	1	33	68	122	33	308	36	4.7	0.9	2	236	19	58	9	33	< 1.5	16	
<b>Site 2</b>																												
0-7	35.2	8.8	0.13	1.4	5.7	0.41	21	18	59	19	2	25	82	99	42	442	27	1.6	0.3	3	237	34	60	< 3.0	21	< 1.5	33	
13-19	34.7	8.9	0.12	1.4	5.8	0.41	14	13	60	15	1	26	78	95	40	405	26	< 0.5	< 0.3	5	235	34	69	46	21	< 1.5	28	
25-31	34.7	8.6	0.11	1.4	5.7	0.33	10	20	52	14	3	25	80	97	44	478	26	< 0.5	0.7	4	255	44	83	33	29	< 1.5	29	
37-43	35.3	9.2	0.11	1.4	5.9	0.33	7	14	59	14	5	30	81	99	43	444	28	1.0	0.3	4	236	43	74	47	53	< 1.5	27	
49-57	35.5	8.5	0.09	1.4	5.4	0.27	< 0.8	19	55	16	6	24	79	99	42	526	27	< 0.5	0.6	4	235	37	64	< 3.0	54	< 1.5	28	
62-70	32.8	8.6	0.11	1.3	5.7	0.83	15	16	71	16	9	27	78	170	39	401	25	1.9	1.0	5	214	43	72	41	31	< 1.5	23	
78-86	35.3	7.9	0.13	1.7	5.5	2.18	2	34	54	20	4	16	86	96	43	293	26	6.0	0.4	3	293	33	73	48	42	< 1.5	22	
94-102	34.1	8.1	0.14	1.6	5.6	2.10	5	45	81	14	3	9	86	86	39	239	25	7.8	1.1	3	256	28	58	64	46	< 1.5	22	
116-124	35.8	7.8	0.14	1.7	4.9	1.63	11	28	63	17	3	10	82	94	39	240	27	7.7	0.4	4	274	32	55	54	19	< 1.5	22	
132-140	35.3	8.0	0.15	1.6	4.7	1.69	15	31	76	11	5	14	81	91	38	251	26	3.4	< 0.3	3	290	33	69	50	40	< 1.5	25	
148-156	39.9	7.2	0.15	1.7	3.8	1.17	8	21	53	10	2	10	75	89	43	311	28	2.1	0.8	3	351	37	79	49	19	< 1.5	23	

Table A9. Major element (%) and trace element ( $\mu\text{g g}^{-1}$ ) concentrations. Sites 8, 7 and 5.

	SiO <sub>2</sub>	Al <sub>2</sub> O <sub>3</sub>	P <sub>2</sub> O <sub>5</sub>	Fe <sub>2</sub> O <sub>3</sub>	TiO <sub>2</sub>	SO <sub>3</sub>	V	Cr	Ni	Cu	Zn	Ga	Ge	As	Rb	Sr	Y	Zr	Nb	Mo	Cd	Sn	Ba	La	Ce	Nd	Pb	
<b>Site 8</b>	%	%	%	%	%	%																						
0-2	61.4	16.2	0.13	5.6	1.3	0.6	130	106	24	12	50	17	1.2	20	73	115	27	311	17	0.8	-0.1	3.3	204	26	60	19	21	
2-4	63.1	15.9	0.12	5.5	1.3	0.6	131	112	25	14	46	18	0.8	21	73	112	29	340	17	0.7	-0.1	3.0	211	26	60	16	20	
4-6	64.2	15.1	0.11	5.3	1.3	0.5	128	126	20	13	42	16	0.6	19	69	116	30	450	17	0.3	-0.1	2.8	230	26	63	21	19	
6-8	65.5	14.9	0.11	5.1	1.3	0.5	131	210	21	15	43	16	1.0	18	69	117	29	407	17	1.2	-0.1	2.9	226	25	60	20	19	
10-12	63.6	15.8	0.12	5.5	1.3	0.4	139	108	22	14	45	18	1.0	21	73	107	28	320	17	0.4	0.2	3.0	209	24	59	18	20	
12-16	64.8	15.2	0.12	5.2	1.3	0.4	136	111	24	47	69	19	1.0	21	75	110	29	306	17	1.1	-0.1	3.5	218	25	60	21	22	
20-24	64.3	15.5	0.12	5.3	1.3	0.4	148	113	25	34	57	19	-0.6	22	74	113	30	338	17	0.3	0.2	3.5	216	28	61	17	21	
32-36	58.9	16.4	0.09	5.4	1.2	1.7	142	112	25	51	66	19	0.9	16	78	158	28	281	16	1.7	-0.1	3.3	188	24	57	20	20	
42-48	55.5	17.4	0.10	6.1	1.2	3.5	141	104	28	39	64	18	1.2	19	78	175	27	248	16	7.4	0.5	3.8	181	25	59	17	20	
54-60	61.7	15.4	0.08	5.5	1.2	3.4	140	107	26	41	58	19	1.0	21	75	152	28	321	16	7.9	0.3	5.2	197	23	59	18	21	
64.5-69	64.5	14.8	0.08	4.9	1.2	2.5	142	118	22	37	58	17	1.2	20	74	142	29	347	16	2.6	0.2	2.8	208	25	60	18	19	
<b>Site 7</b>																												
0-2	65.3	13.8	0.10	4.64	1.2	0.3	108	97	18	16	45	14	0.8	16	63	105	31	442	16	-0.6	0.2	3.2	195	28	62	20	20	
4-6	63.9	14.1	0.10	4.61	1.2	0.3	123	104	22	20	49	18	0.8	19	71	94	33	427	18	0.5	0.1	3.9	202	28	65	21	21	
8-10	63.5	14.2	0.10	4.73	1.1	0.3	126	99	21	18	48	17	0.5	20	69	100	30	399	17	0.6	0.2	3.7	193	27	63	18	22	
12-16	65.7	13.1	0.08	4.35	1.1	0.4	119	94	19	19	44	16	1.0	21	69	106	31	405	17	1.8	0.2	4.0	221	30	69	22	20	
16-20	59.3	13.4	0.07	4.18	1.0	0.3	113	88	19	30	52	15	1.0	19	62	122	29	385	15	3.1	-0.1	3.8	171	27	60	15	18	
24-28	50.4	15.0	0.08	4.68	0.9	0.5	98	71	18	44	62	14	-0.6	19	60	118	22	234	12	8.1	-0.1	3.1	136	20	45	16	18	
32-35.5	43.2	15.3	0.07	4.44	0.7	0.6																						
<b>Site 5</b>																												
0-2	57.3	17.1	0.15	5.75	1.6	0.3																						
2-4	57.6	17.0	0.17	5.75	1.7	0.3																						
6-8	56.2	18.0	0.15	5.60	1.4	0.2																						
10-12	56.9	17.9	0.13	5.34	1.5	0.3																						
12-16	58.3	17.3	0.13	5.22	1.5	0.3																						
20-24	60.4	17.1	0.10	4.60	1.3	0.4																						
28-32	54.6	18.4	0.09	5.67	1.2	0.7																						
36-40	55.0	19.7	0.07	5.85	1.2	0.7																						
44-48	56.2	19.4	0.06	5.58	1.2	0.6																						